Response and Sensitivity of the Stable Boundary Layer to Added Downward Long-wave Radiation

Dick McNider

University of Alabama in Huntsville

Thanks to: G.J. Steeneveld, B. Hotlslag, S.Mackaro, A.. Biazar, R. Pielke, J. Christy, J.Hnilo

UAH

"Global" Surface Temperature

Made up of 5000-7000 stations around the world. Most based data sets only carry a Tmean which is the average of the original maximum (Tmax) and minimum (Tmin)

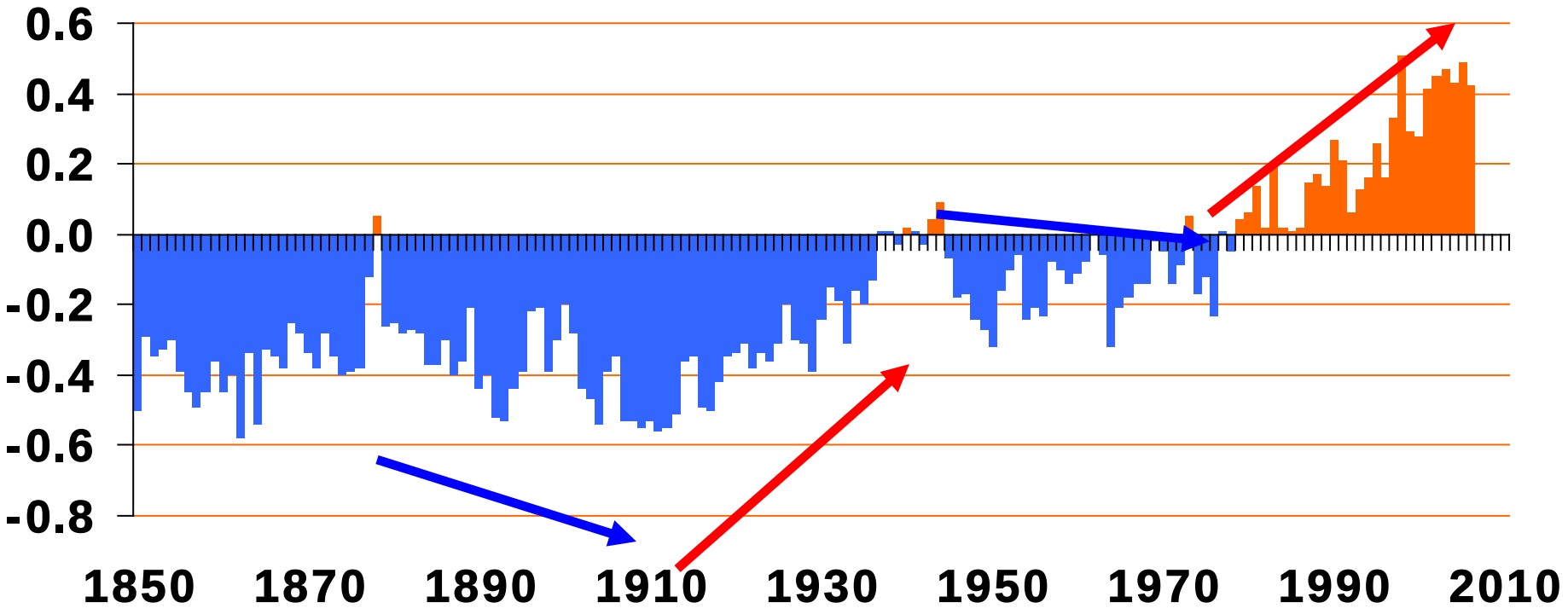

UAH

NOAA NCDC GHCN Land Trends

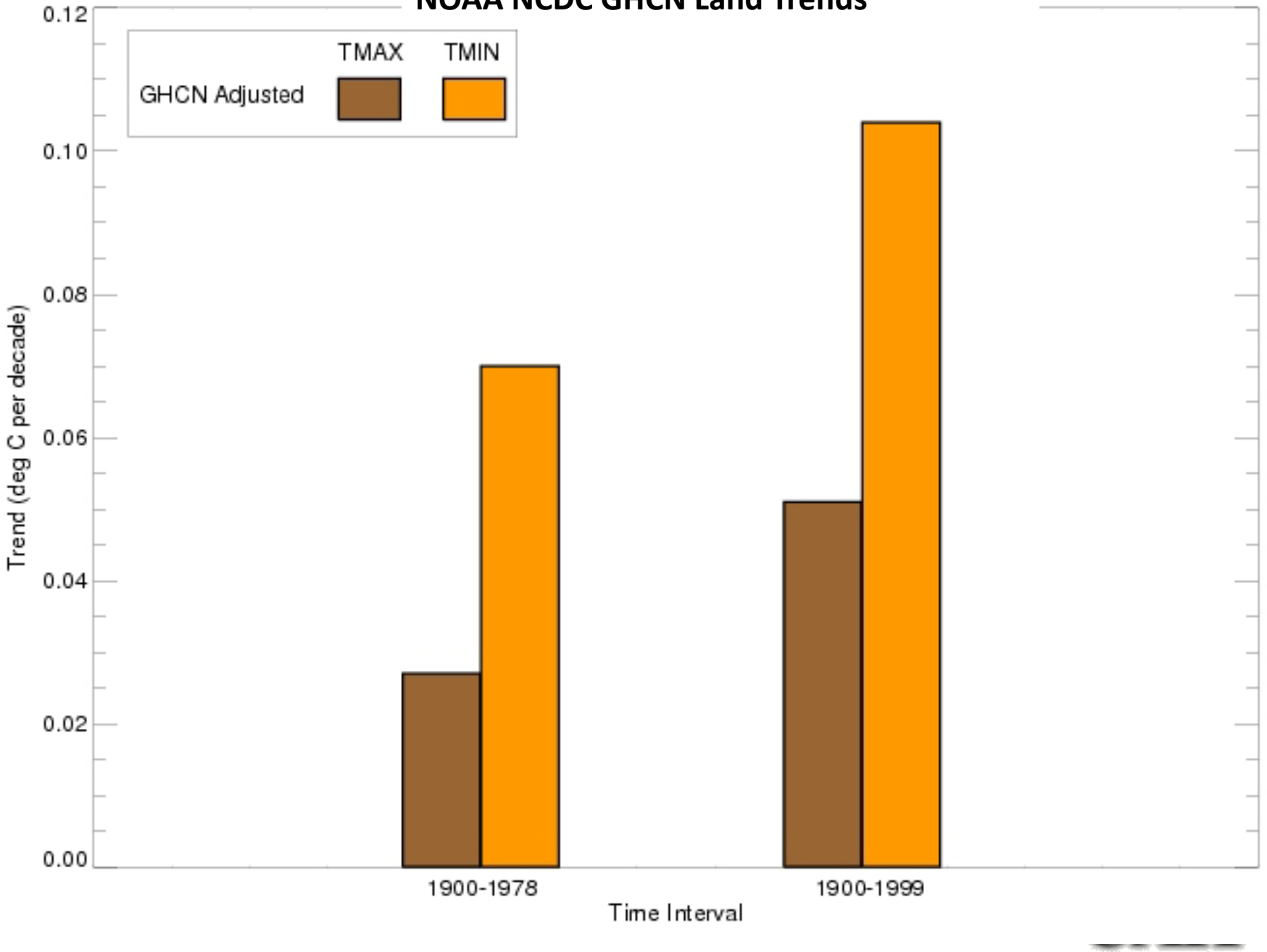

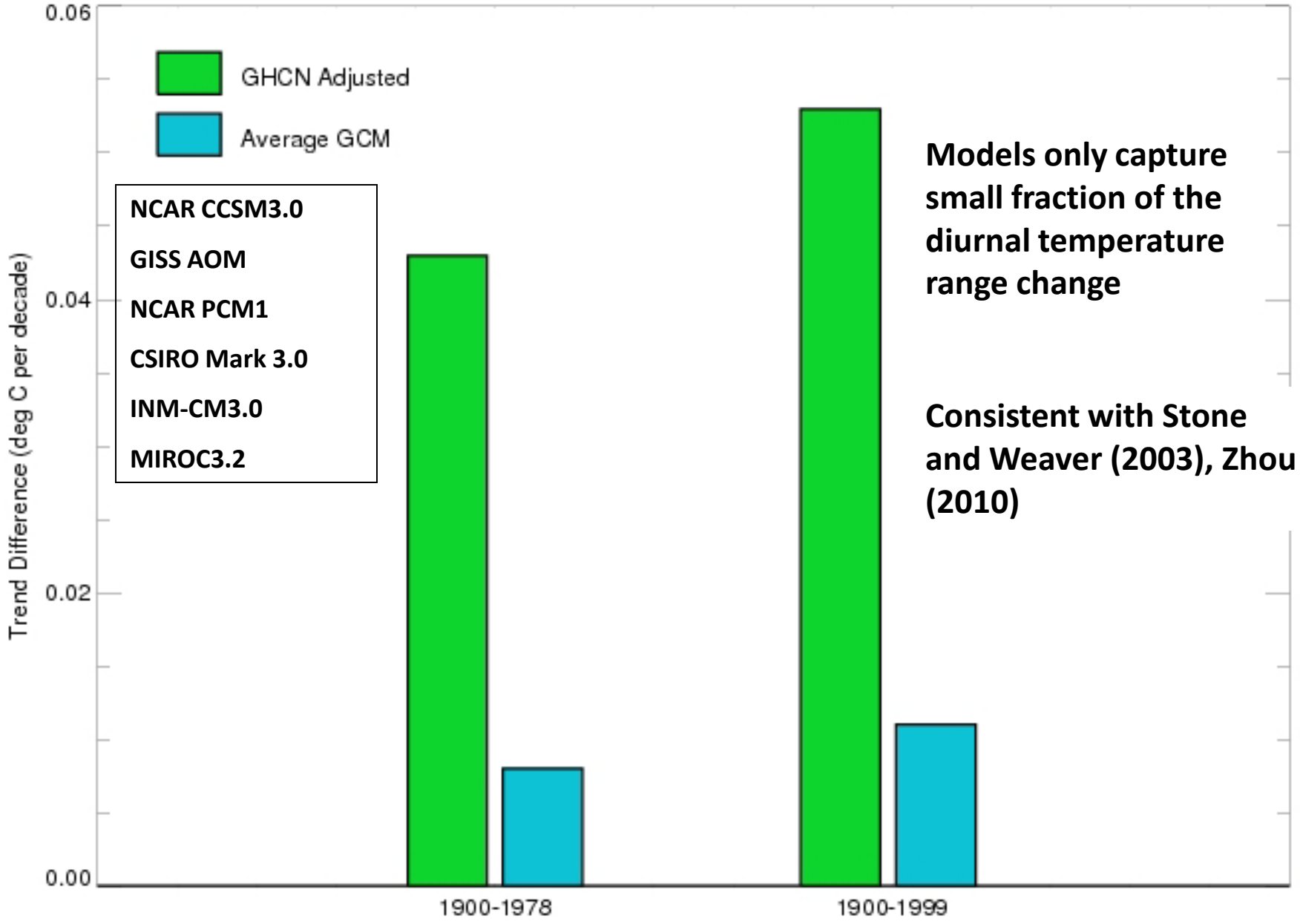
GHCN and Average GCM Trend Differences (TMAX - TMIN)
for Global Land Surface Temperatures
0.06
0.04
0.02
0.00
Trend Difference (deg C per decade)
GHCN Adjusted
Average GCM
NCAR CCSM3.0
GISS AOM
NCAR PCM1
CSIRO Mark 3.0
INM-CM3.0
MIROC3.2
1900-1978
1900-1999
Models only capture small fraction of the diurnal temperature range change
Consistent with Stone and Weaver (2003), Zhou (2010)

This asymmetry in warming is one of the most significant signals in the observed climate record

The reasons for this asymmetrical rise have been subject to considerable debate

1. **Increased cloudiness (Dai et al.1999)**
2. **Urbanization (Balling and Idso, 2002, Gallo et al. 1999)**
3. **Surface moisture/irrigation (Durre and Wallace, 2001, Christy et al. 2005)**
4. **Aerosols (Charlson et al. 1992, Dai et al. 1997)**
5. **Contrails (Travis et al. 2004)**
6. **Stable boundary layer dynamics Walters et al. 2007 *GRL***

UAH

In order to examine the dynamics of the stable boundary layer and its sensitivity to external forcing such as downward radiation from greenhouse gases we employ a one-dimensional model (column model).

$$\begin{aligned}
\frac{\partial u}{\partial t} &= f_{co}(v - v_G) + \frac{\partial}{\partial z}\left(K_m(z, u_z, v_z, \theta_z)\frac{\partial u}{\partial z}\right), \\
\frac{\partial v}{\partial t} &= f_{co}(u_G - u) + \frac{\partial}{\partial z}\left(K_m(z, u_z, v_z, \theta_z)\frac{\partial v}{\partial z}\right), \\
\frac{\partial \theta}{\partial t} &= R_c(\theta) + \frac{\partial}{\partial z}\left(K_h(z, u_z, v_z, \theta_z)\frac{\partial \theta}{\partial z}\right),
\end{aligned} \tag{1.1}$$

Coupled with a simple slab energy budget for the surface

$$\begin{aligned}
\frac{d\theta_g(t)}{dt} = \frac{1}{C_g}\big(I_1(\theta)|_{z=z_0} - \sigma\theta_g^4(t) - H_0(z, u_z, v_z, \theta_z)|_{z=z_0}\big) \\
- \kappa_m(\theta_g(t) - \theta_m), \qquad t > 0,
\end{aligned} \tag{1.2b}$$

UAH

Rather than solve the column equations numerically in the past we truncated the system to two layers

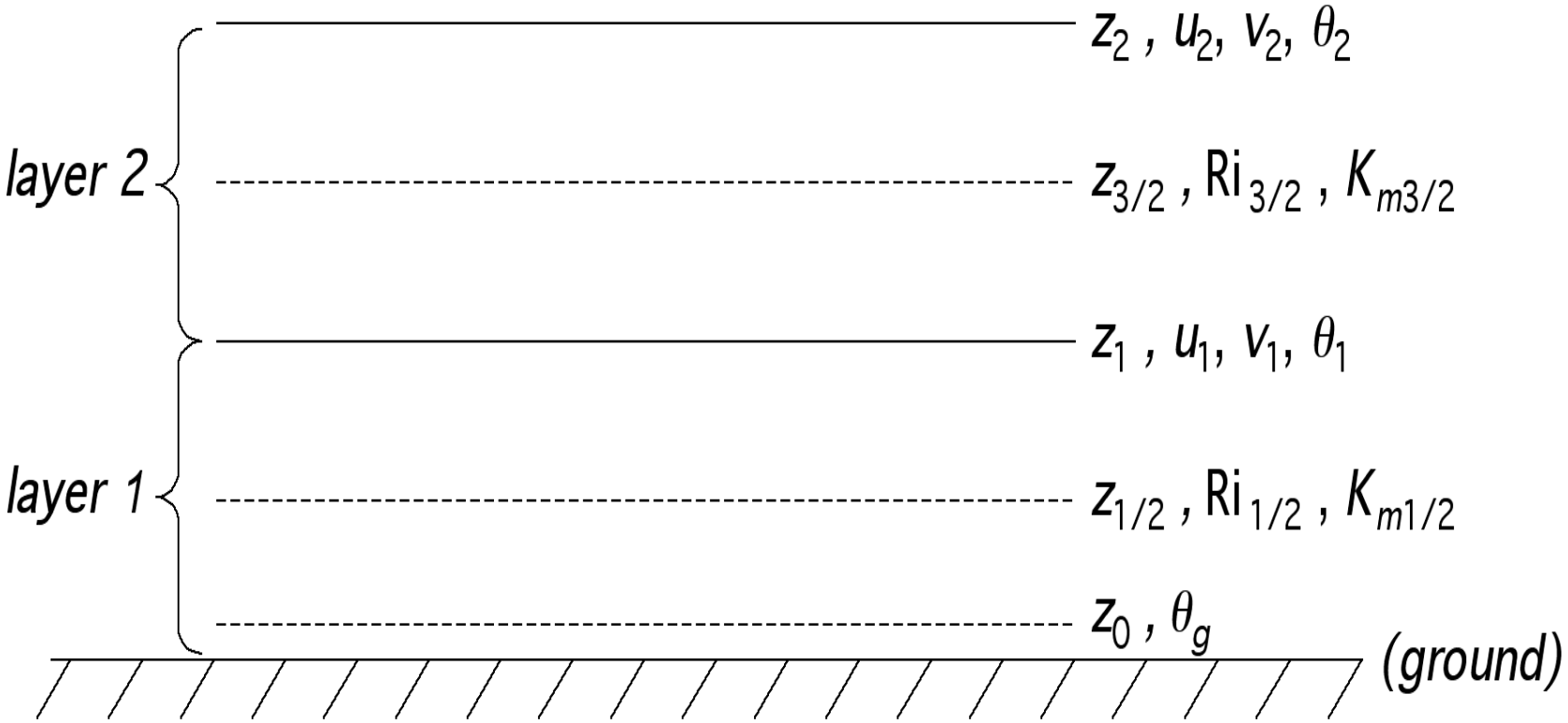

Therefore we reach a system of 4 first order ODEs (a two-layer model):

$$
\begin{aligned}
\frac{du_1}{dt} &= f_{co}(v_1 - v_G) + \frac{1}{z_{3/2} - z_{1/2}}\left(\frac{K_{m,3/2}(u_2 - u_1)}{z_2 - z_1} - u_*^2 \cos(\psi)\right), \\
\frac{dv_1}{dt} &= f_{co}(u_G - u_1) + \frac{1}{z_{3/2} - z_{1/2}}\left(\frac{K_{m,3/2}(v_2 - v_1)}{z_2 - z_1} - u_*^2 \sin(\psi)\right), \\
\frac{d\theta_1}{dt} &= \frac{1}{z_{3/2} - z_{1/2}}\left(\frac{K_{h,3/2}(\theta_2 - \theta_1)}{z_2 - z_1} - u_*\theta_*\right), \\
\frac{d\theta_g}{dt} &= \frac{1}{C_g}(I_1 - \sigma\theta_g^4 - H_0) - \kappa_m(\theta_g - \theta_m),
\end{aligned}
\tag{5.1}
$$

with initial conditions

$$
u_1(0) = u_G, \quad v_1(0) = v_G, \quad \theta_1(0) = \theta_A. \tag{5.2}
$$

Where u_*, θ_* are the friction velocity and friction temperature, given by

$$
u_* = \frac{\kappa\sqrt{f_m(Ri_{1/2})}\sqrt{u_1^2 + v_1^2}}{ln(z_1/z_0)}, \quad \theta_* = \frac{\kappa(\theta_1 - \theta_g)f_h(Ri_{1/2})}{\sqrt{f_m(Ri_{1/2})}ln(z_1/z_0)}, \tag{5.3}
$$

Use of Nonlinear Analysis to Explore Climate Sensitivity

Rather than integrating the ODEs numerically we employ tools in nonlinear analysis to explore the behavior of the system of equations. The primary tools are numerical continuation that can trace out the equilibrium bifurcation diagram, determine special bifurcation points and compute the eigenvalues of the system as a function of the bifurcation parameters.

McNider, R.T., D.E. England, M.J. Friedman and X. Shi, 1995: On the predictability of the stable boundary layer. *J. Atmos. Sci.*

Shi, X., McNider, R.T., D.E. England, M.J. Friedman, W.Lapenta, B. Norris, 2005: On the behavior of the stable boundary layer and role of initial conditions. *Pure Appl. Geophys. 162, 1811-1829*

Walters, J., R. McNider,, X.Shi, W. Norris, J. Christy, 2007: Positive temperature feedback in the stable boundary layer. *Geophys. Res. Lett.*, 34,

UAH

Non-linearity enters through turbulent mixing terms

$K_m = K_h = f_m(\mathrm{Ri})\, l^2 s$

$$f_m(\mathrm{Ri}) = \begin{cases} \left(\dfrac{\mathrm{Ri}_c - \mathrm{Ri}}{\mathrm{Ri}_c} \right)^2, & 0 < \mathrm{Ri} < \mathrm{Ri}_c \\ 0, & \mathrm{Ri} \geq \mathrm{Ri}_c \end{cases}$$

England and McNider 1995 BLM

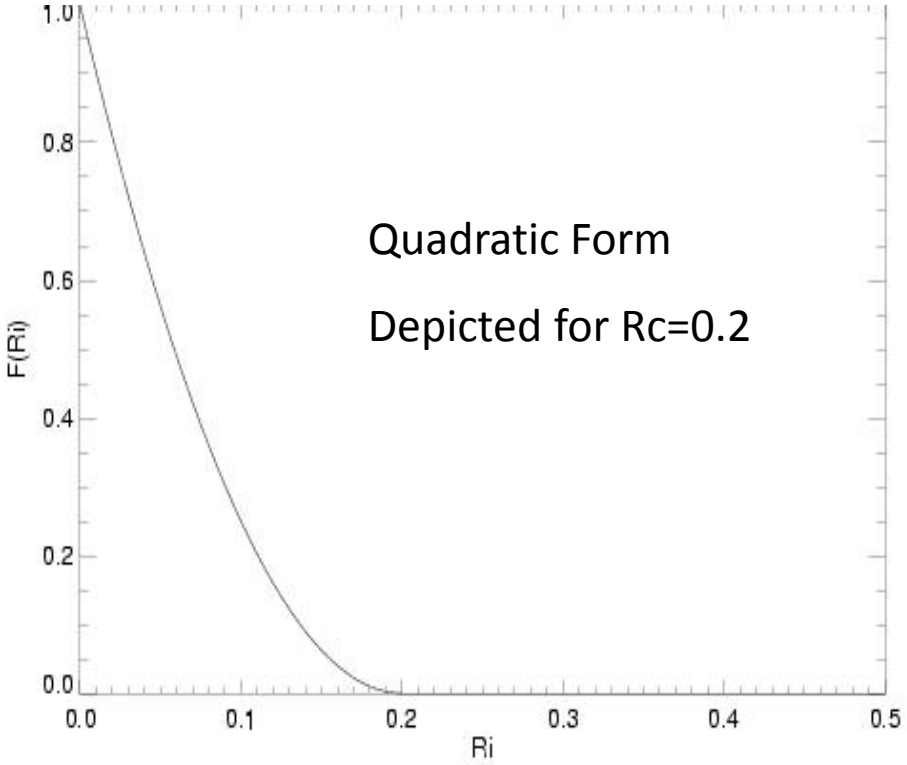

Quadratic Form

Depicted for Rc=0.2

UAH

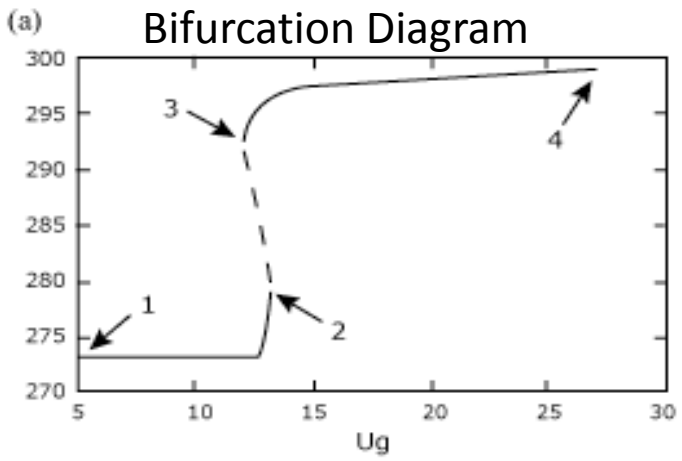

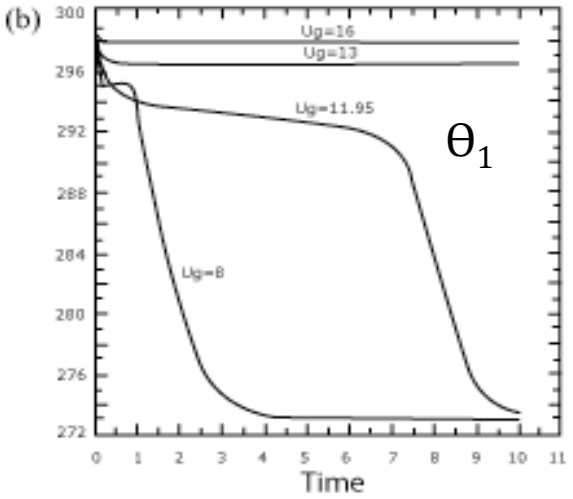

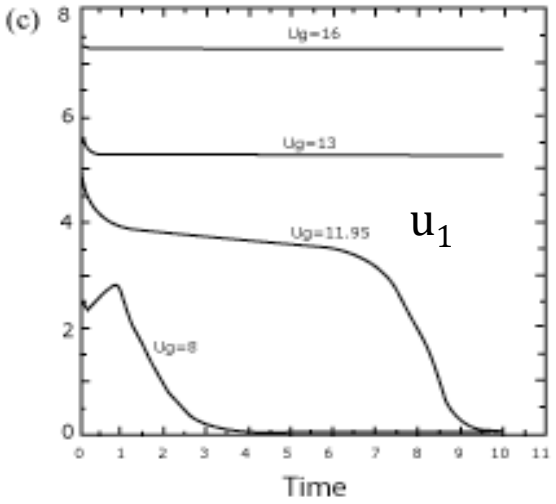

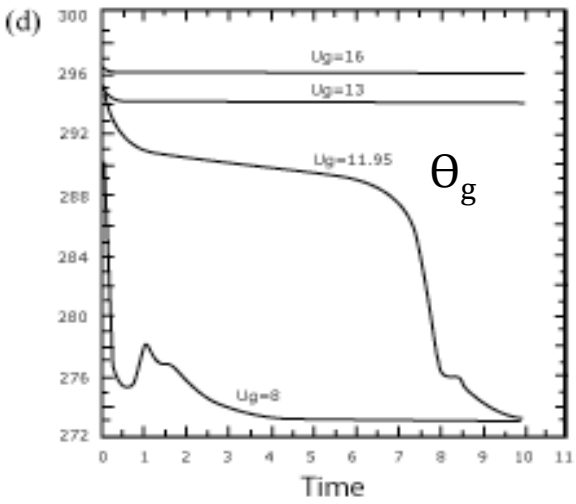

Shi et al 2005

UAH

t

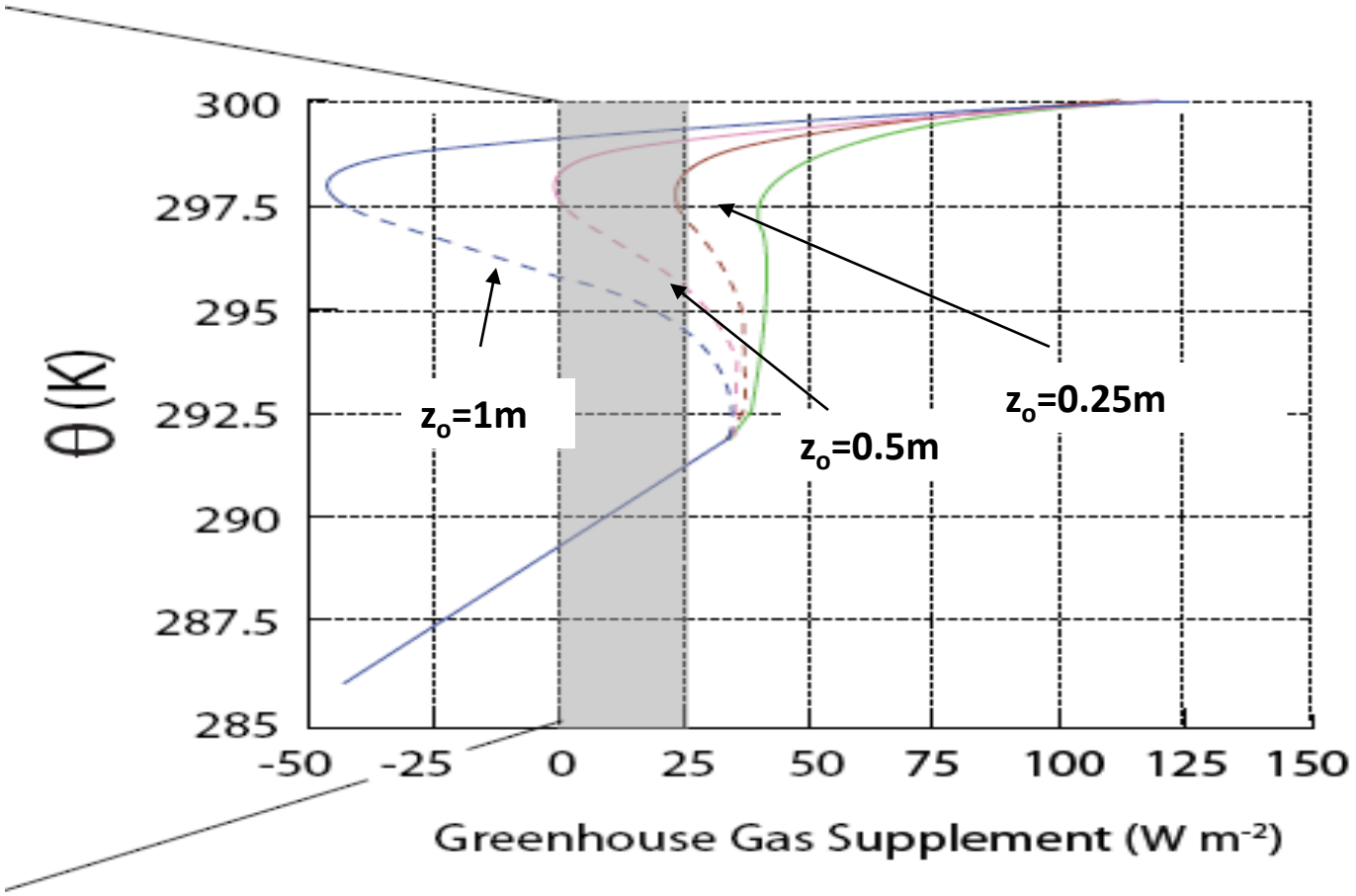

Moderate Winds (7 m/s)

nt (W m^{-2})

Increases in downward radiation act to make the stable boundary less stable

This decreased stability in certain parameter spaces causes the surface to be more connected with the air aloft leading to enhanced warming

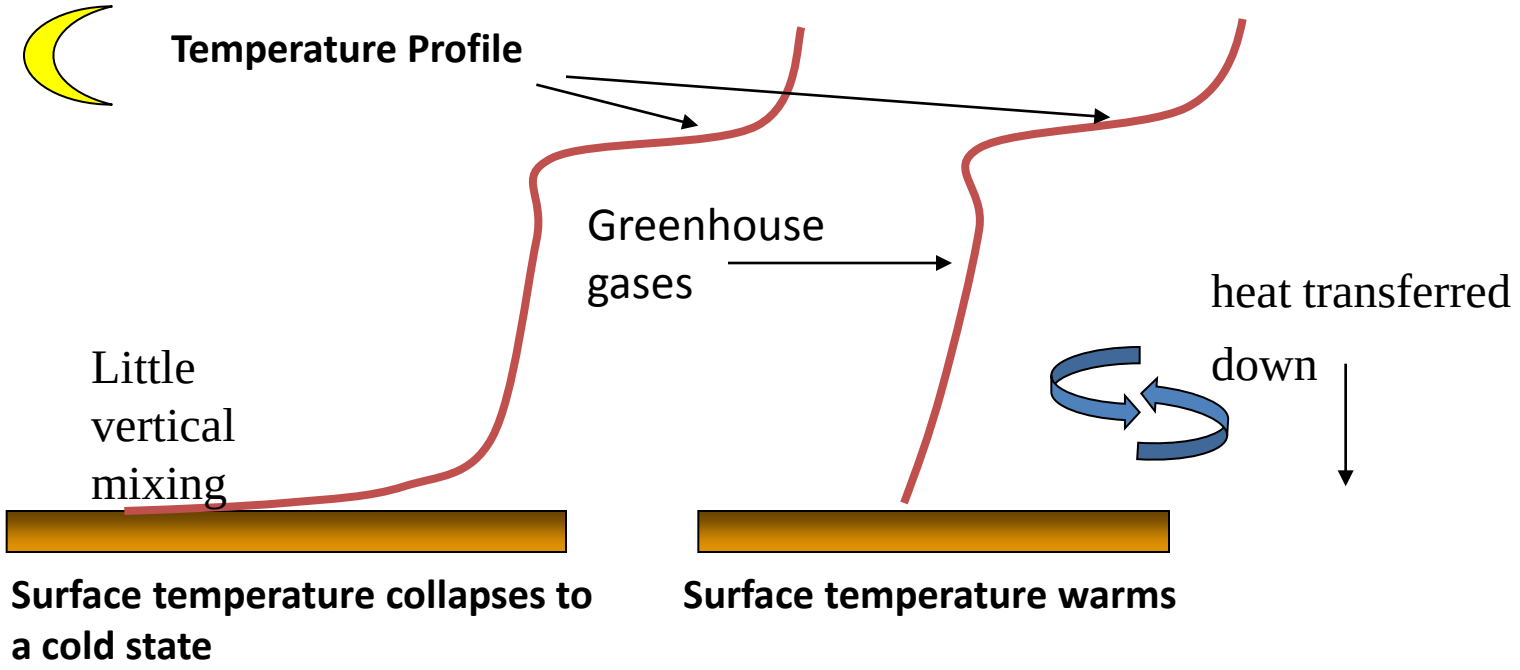

Thus, this acts as a positive climate feedback in that slight changes in downward radiation can lead to large changes in temperature.

However, it is not a net energetic increase but only a redistribution of heat !

UAH

However, the field of non-linear dynamics is littered with exotic behavior that is found in simpler models but not carried into more complete models.

For example *Lorenz 1995* in a discussion on atmospheric predictability noted that “prediction errors in chaotic systems tend to amplify less rapidly on average as the system gets larger”. The additional degrees of freedom tend to smooth or damp the rate at which individual perturbed states depart over time.

So here we will examine the response of the stable boundary layer to added downward long-wave energy using a more complete column model.

UAH

England and McNider 1995
BLM Quadratic Stability Function

Fu and Liou, 1993 multi-band band radiation code

Multi-layers – grid spacing ~ 2m

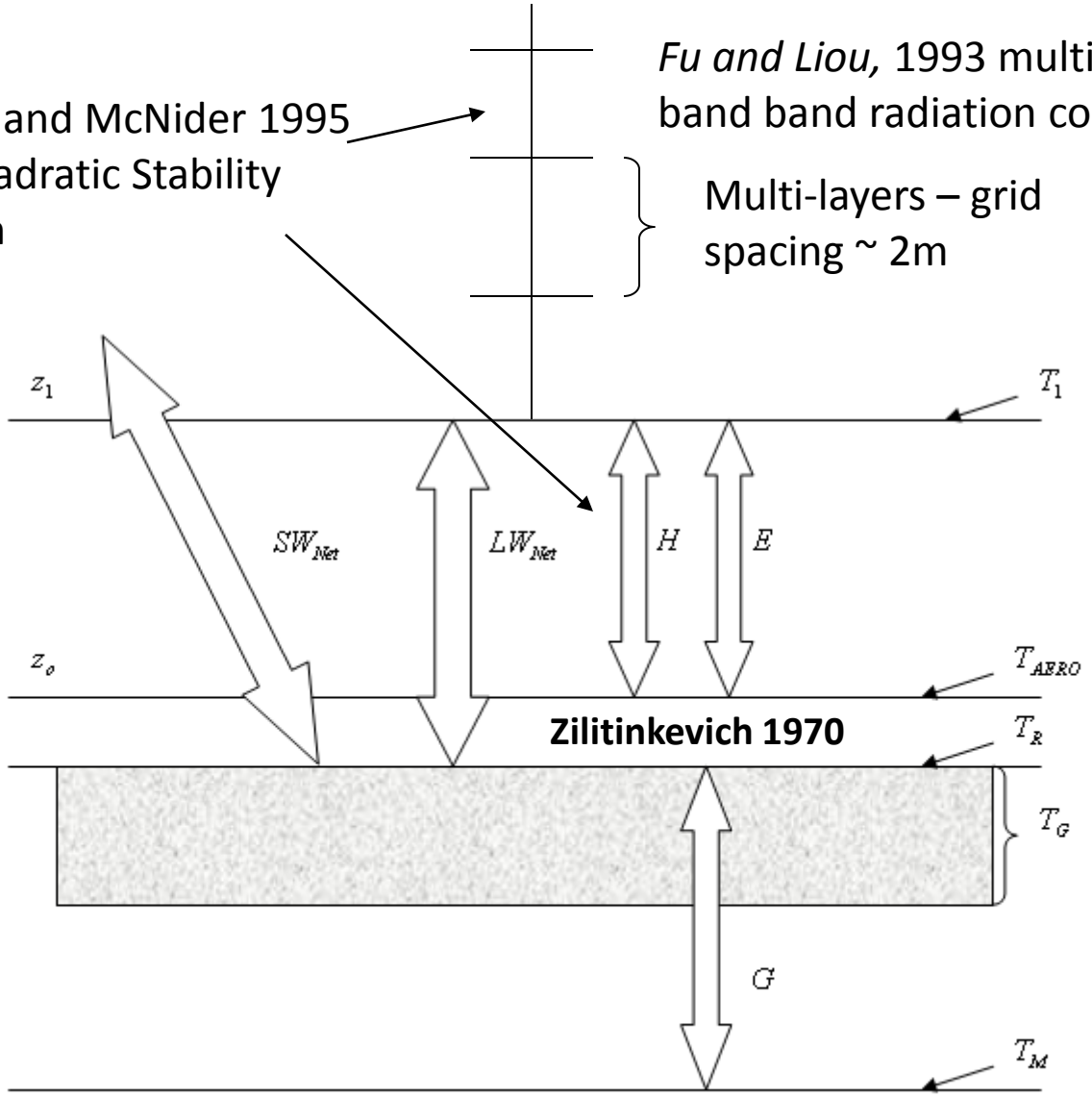

Figure 2 Schematic of a land surface to boundary layer interface that follows the traditional bulk aerodynamic formulation of surface layer fluxes.

UAH

APPENDIX

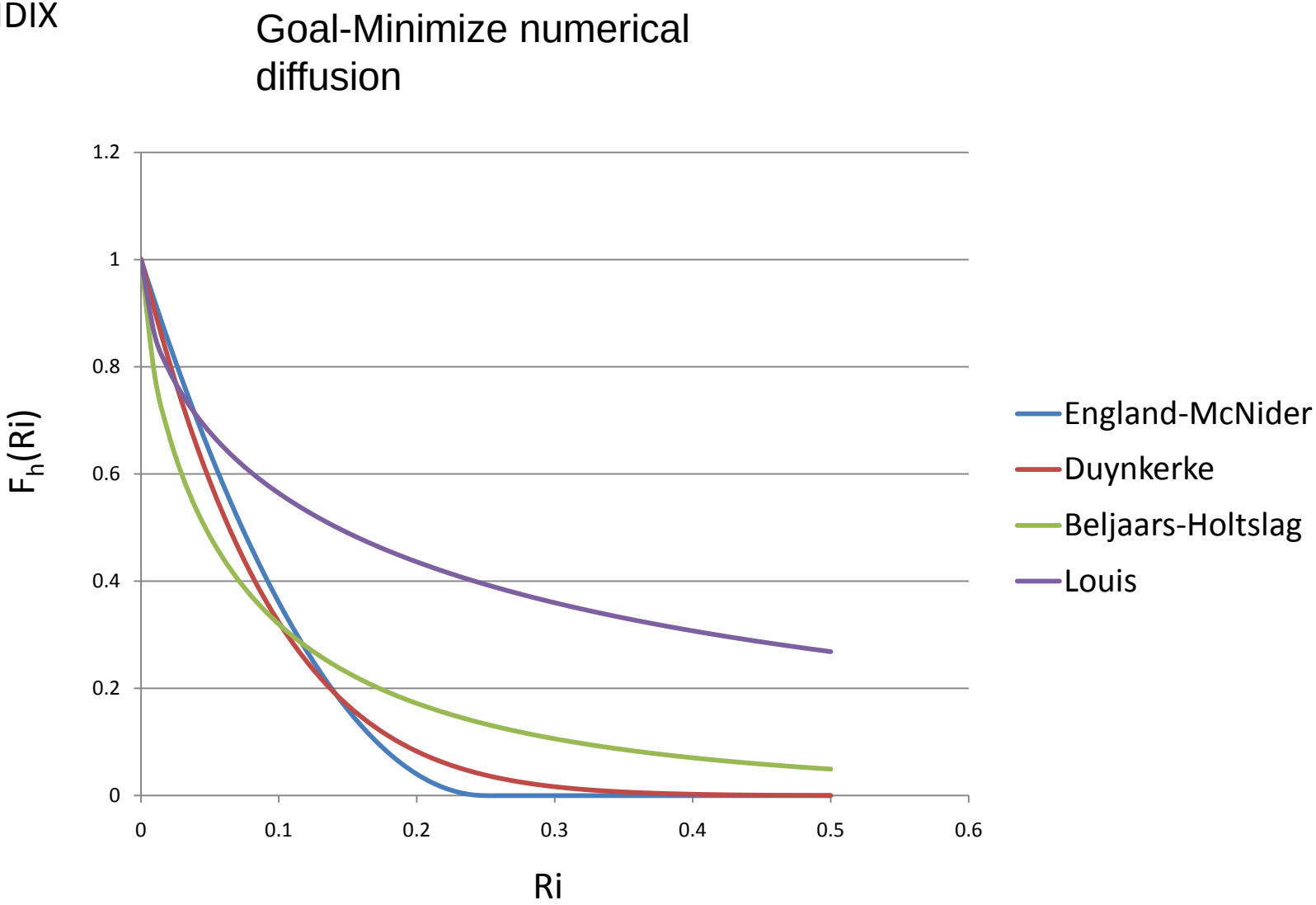

Figure 2A: Stability functions used in the present paper. Ri is the gradient Richardson Number. See England and McNider 1995, Duynkerke 1991, Beljaars and Holtslag 1991 and Louis 1979. Duynkerke, Beljaars and Holtslag and Louis represent curve fits to the original parameterization. See also Van de Weil et al. 2002a

UAH

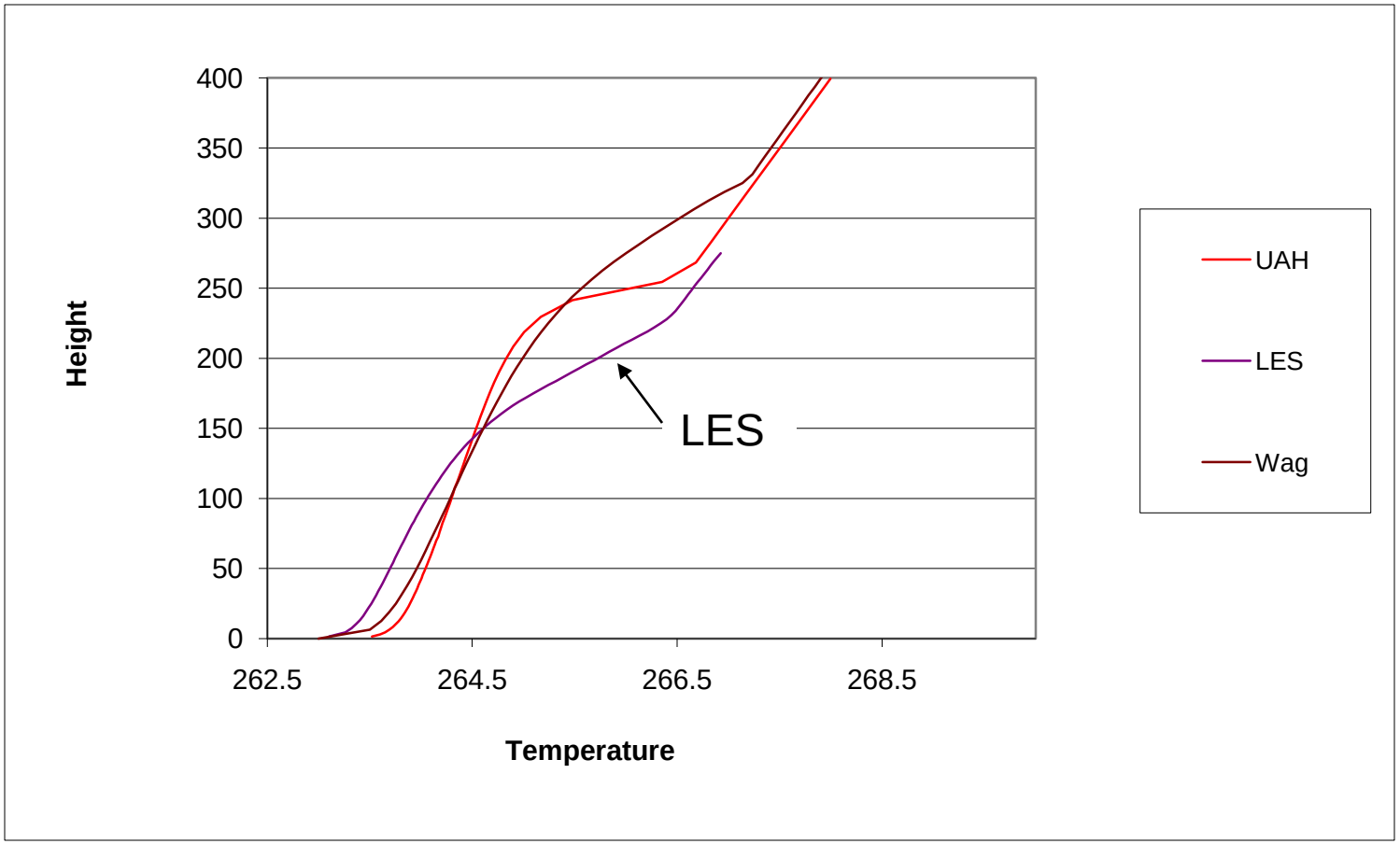

Figure 2: *A posteriori* comparison of the present model (UAH) against the GABLS1 single column model inter-comparison (see Cuxart et al 2005.) LES came from the LES ensemble, WAG is the Wageningen model (see Steeneveld 2006). The B-H and Louis curves are runs with the UAH model using the Beljaars-Holtslag stability function and the Louis stability function.

UAH

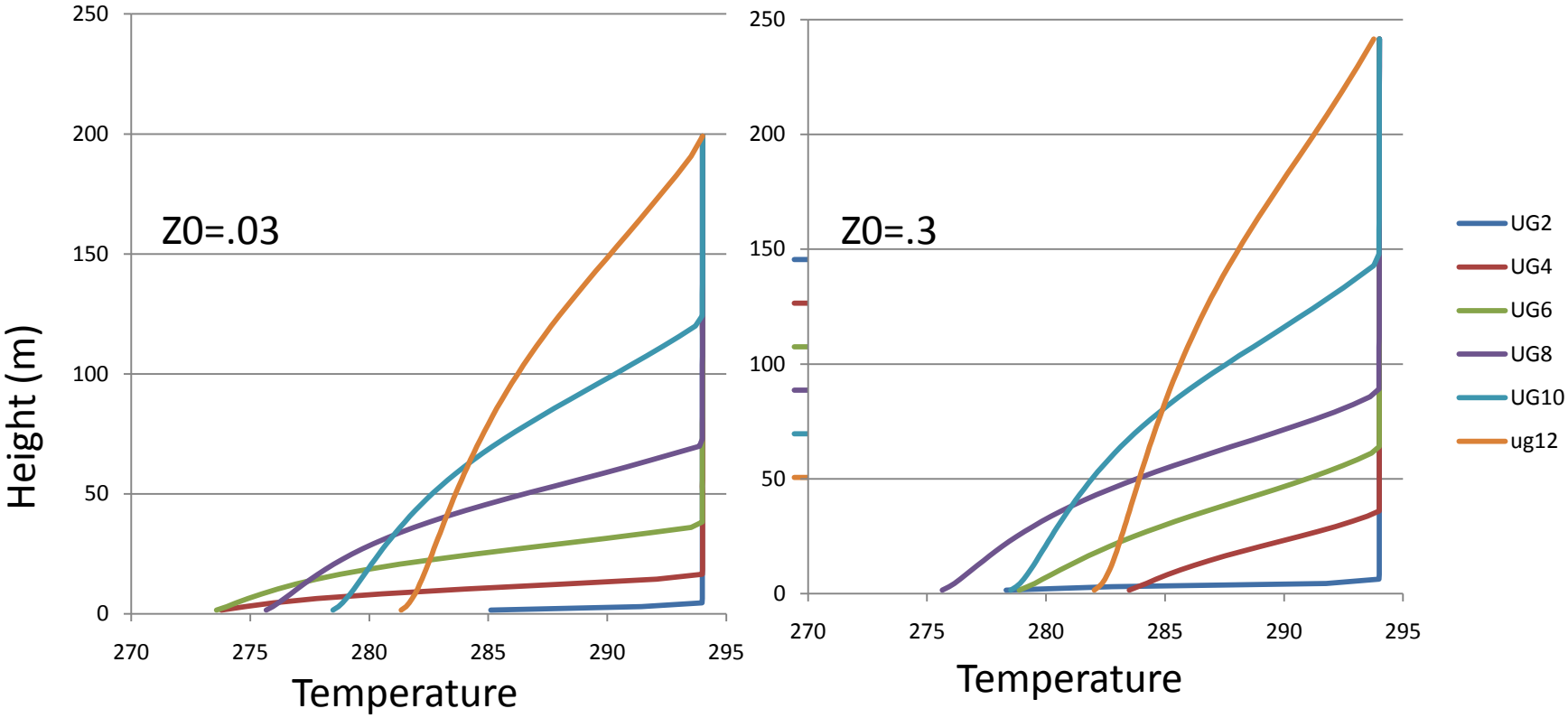

Figure 4: Vertical profiles of temperature for different imposed geostrophic velocities for the UAH model with no clear air radiative forcing.

Added Downward Long-wave Sensitivity Experiments

Added downward long-wave (DLW) energy can come from increased greenhouse gases, water vapor, aerosols, cloudiness, jet contrails.

To make the experiments we added 4.8 Watts of longwave down in the model (after long-wave was calculated from radiation scheme).

The 4.8 Watts came from Steeneveld et al. 2010 in an increased CO_2 study.

Total downward long-wave in the column model comes either from a simple downward radiation model used in the dynamical studies model

$$I_1 \equiv I_1(\theta)|_{z=z_0} = 0.67\sigma(1670Q_a)^{0.08}\theta^4|_{z=z_0}$$

or from a complete modern *Fu and Liou,* 1993 multi-band band radiation code.

UAH

To first order temperature response to IR forcing should depend on boundary layer height

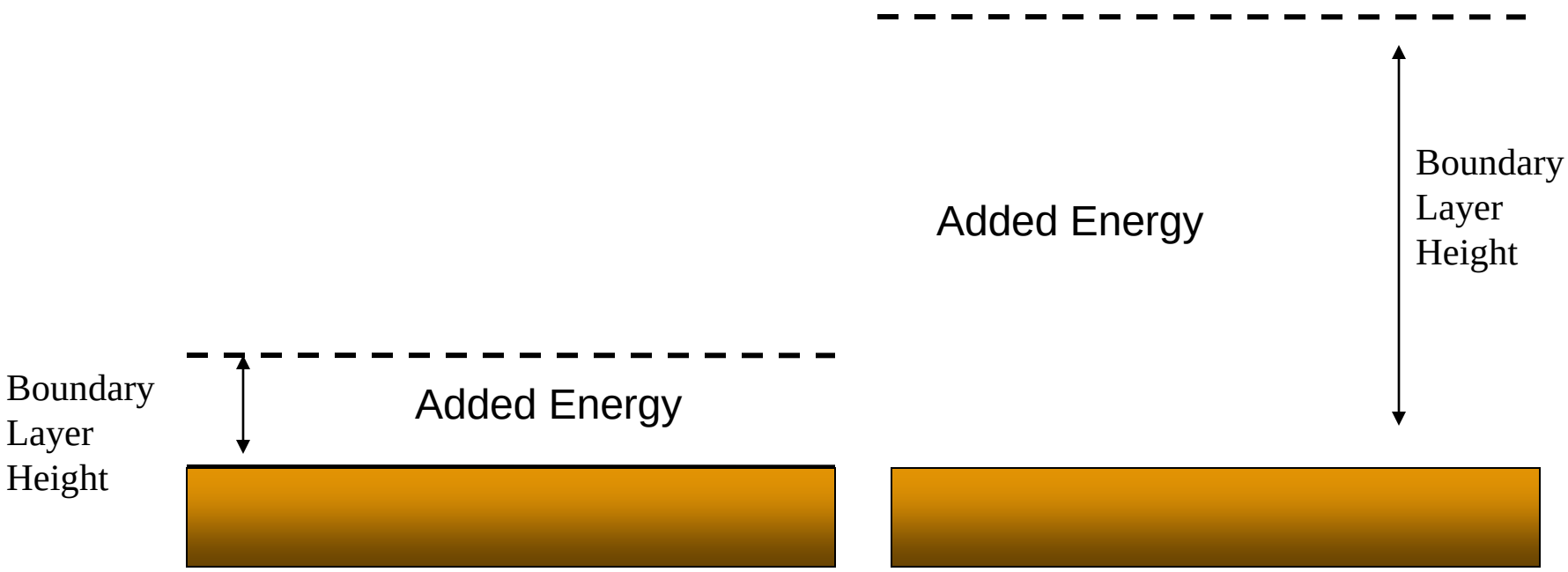

For a given IR forcing warming will depend inversely (but perhaps not linearly) on boundary layer depth. Thus, temperature response will be greater at night than day (Eastman et al. 2001, Esau 2008)

UAH

However, for added IR to heat the atmosphere it must first heat the surface and this heat be transferred to the atmosphere through turbulent sensible heat flux.

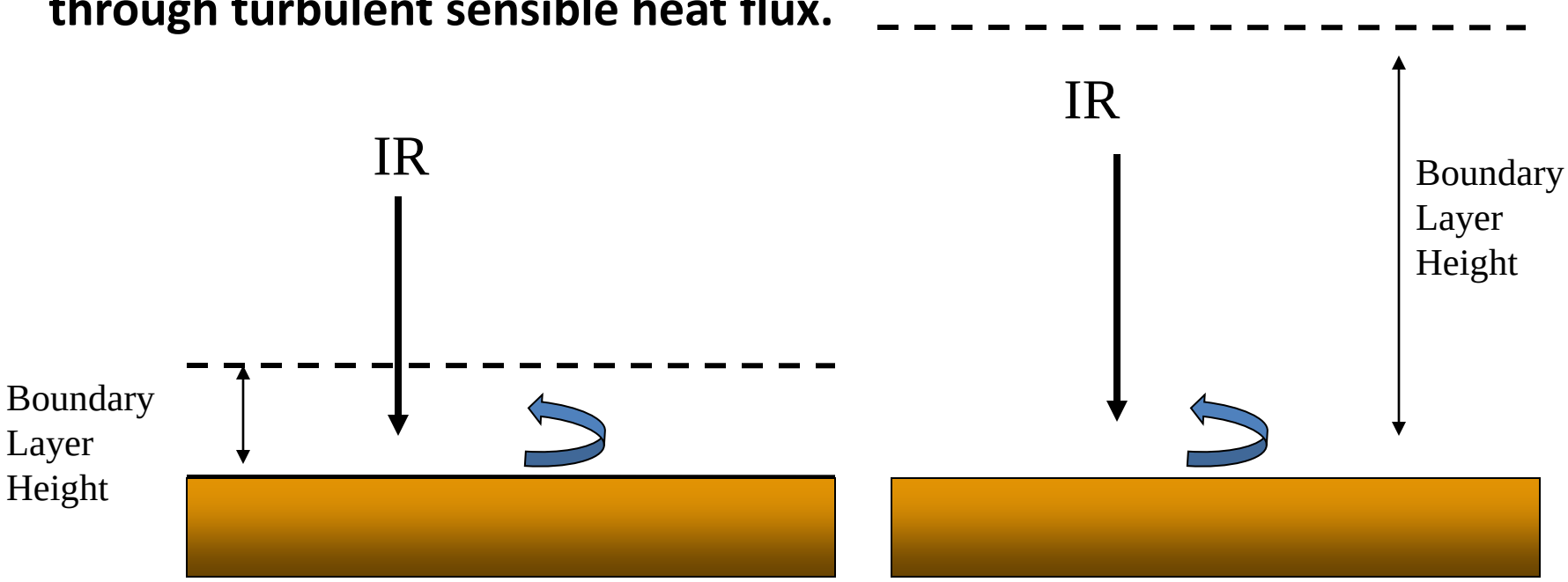

Steeneveld et al 2010 showed that for the stable boundary layer that the heating was independent of boundary layer height (which increases with wind speed) because of the competing effect of sensible heat flux.

UAH

Added Sensible Turbulent Heat Flux

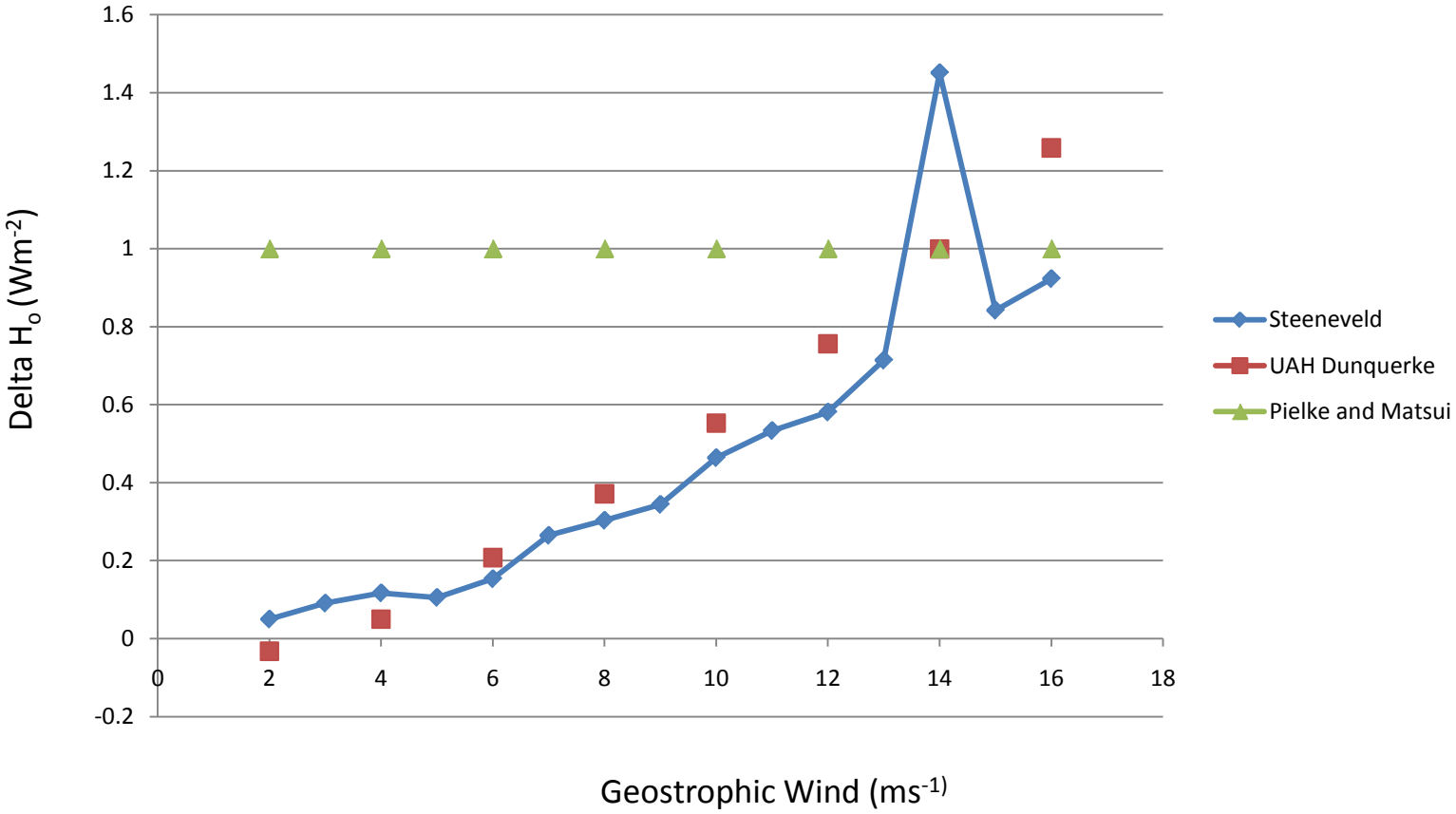

UAH

CASES99 Soils, z_0 =.03m

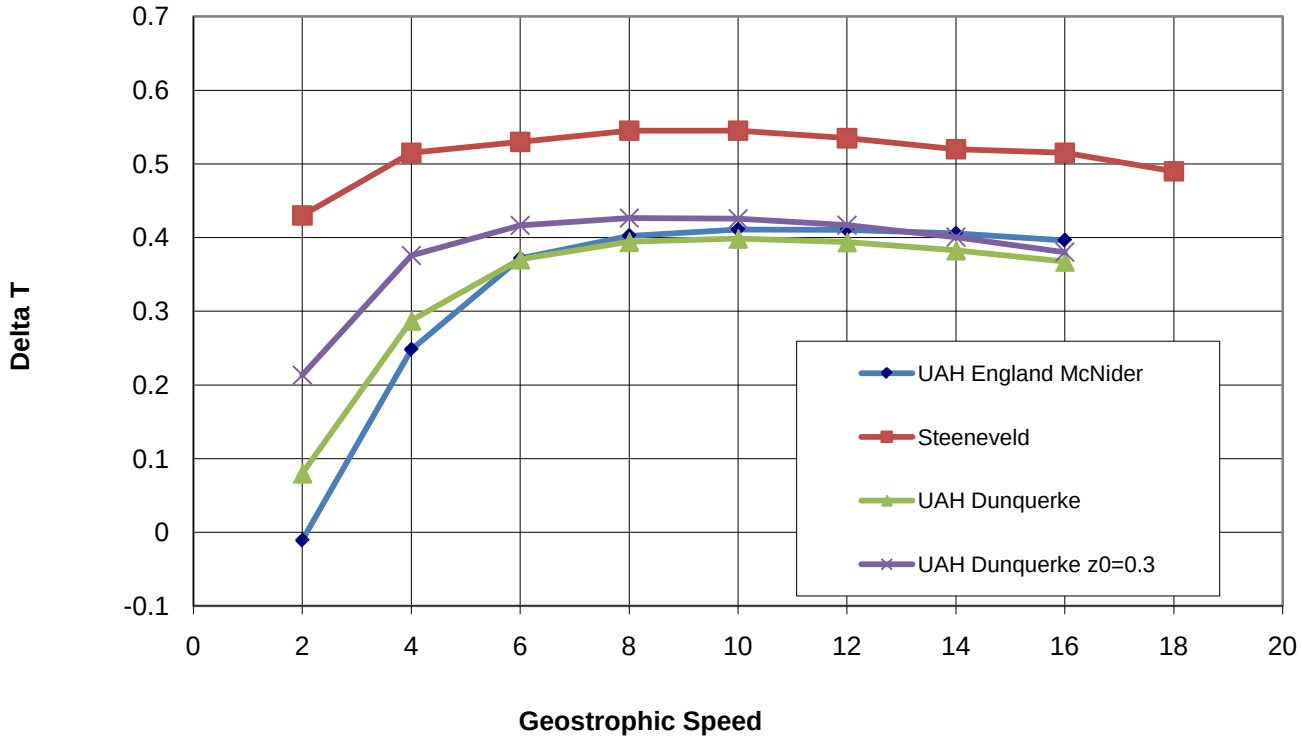

Figure 13: Differential heating - added GHG energy – base case versus wind speed for the Steeneveld soils case with clear air radiational forcing.

Dry sandy soil without clear air radiation, z0=.3m

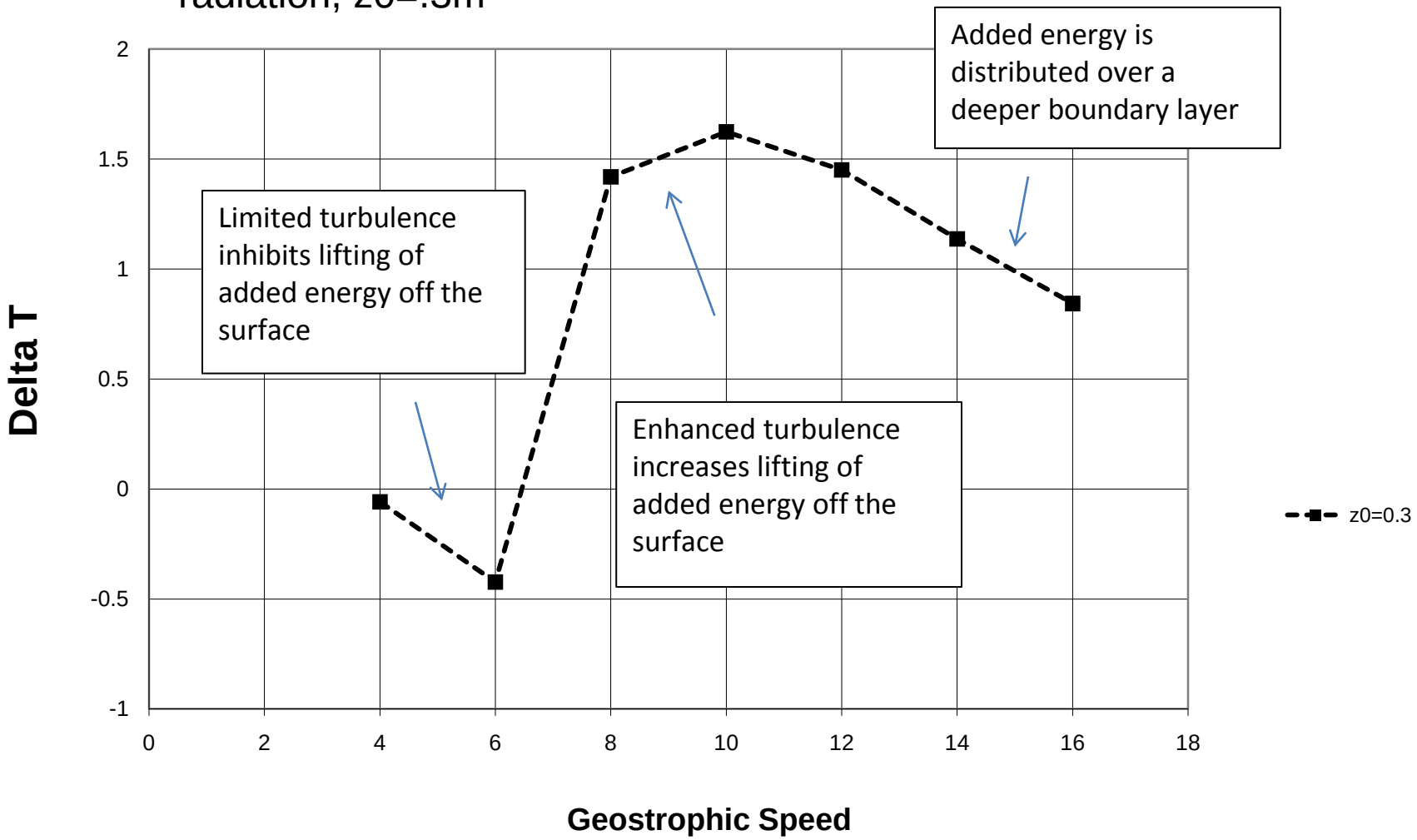

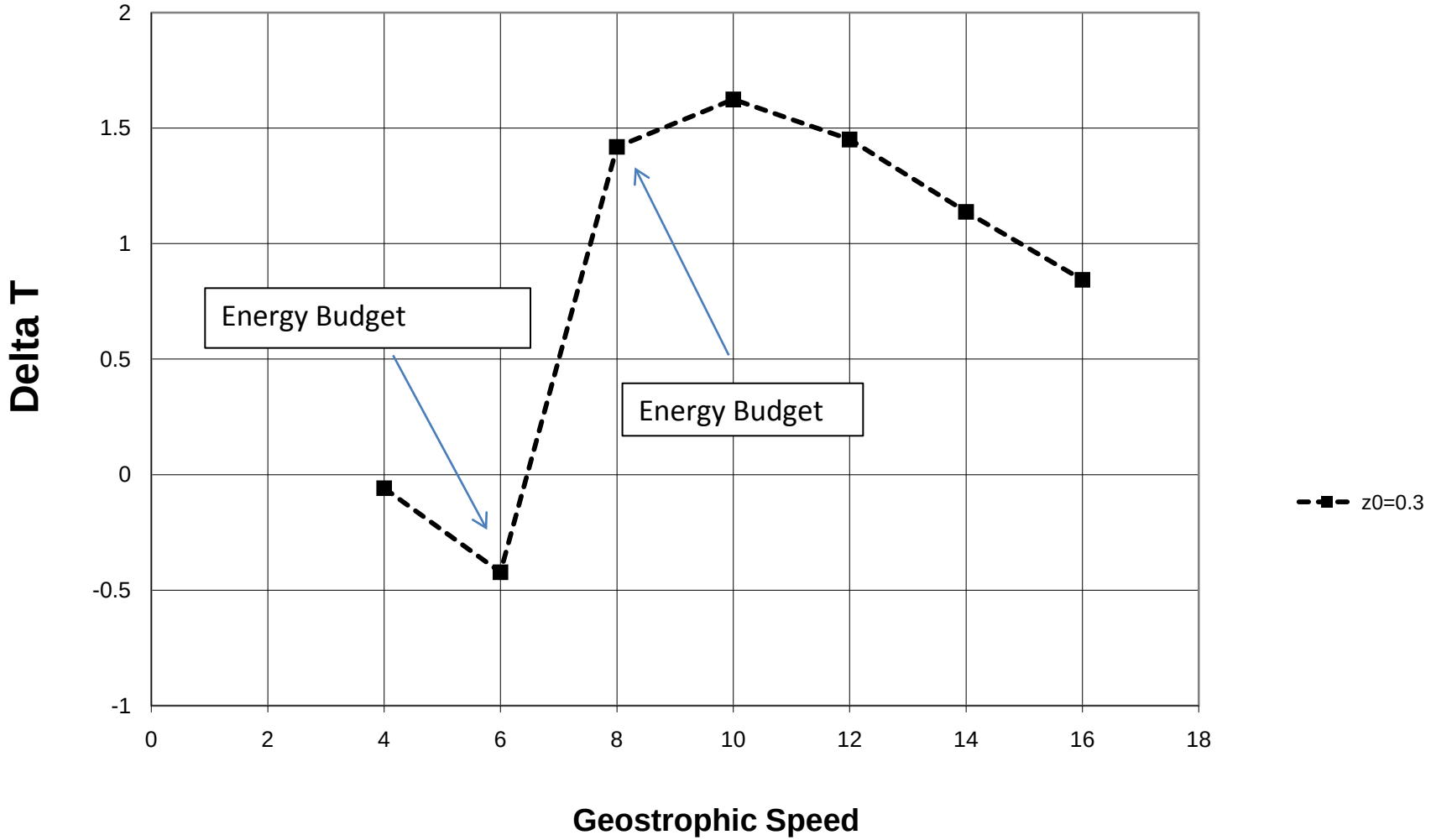
Delta T
2
1.5
1
0.5
0
-0.5
-1
0
2
4
6
8
10
12
14
16
18
Energy Budget
Energy Budget
Geostrophic Speed
z0=0.3

Energy Budgets

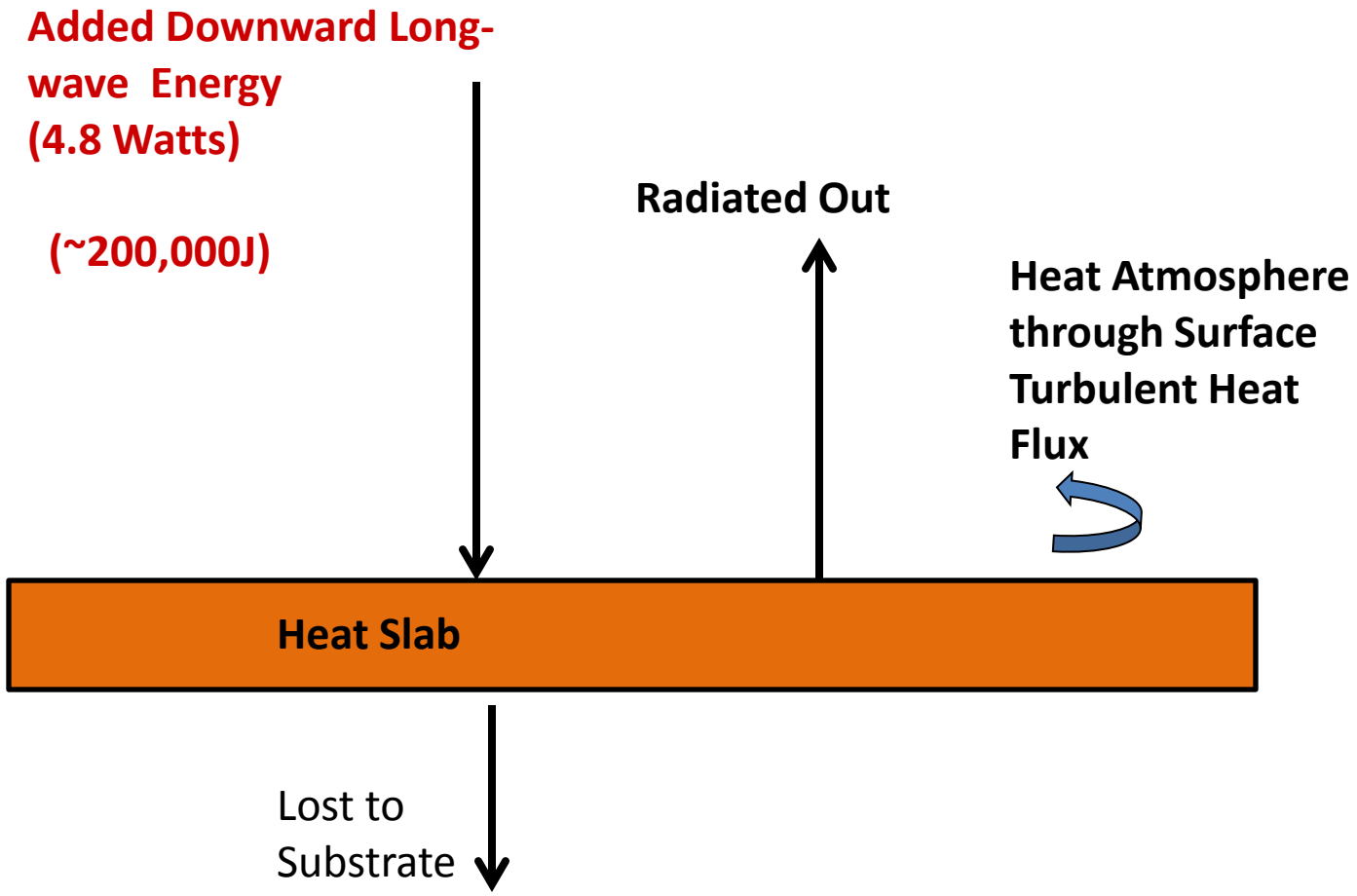

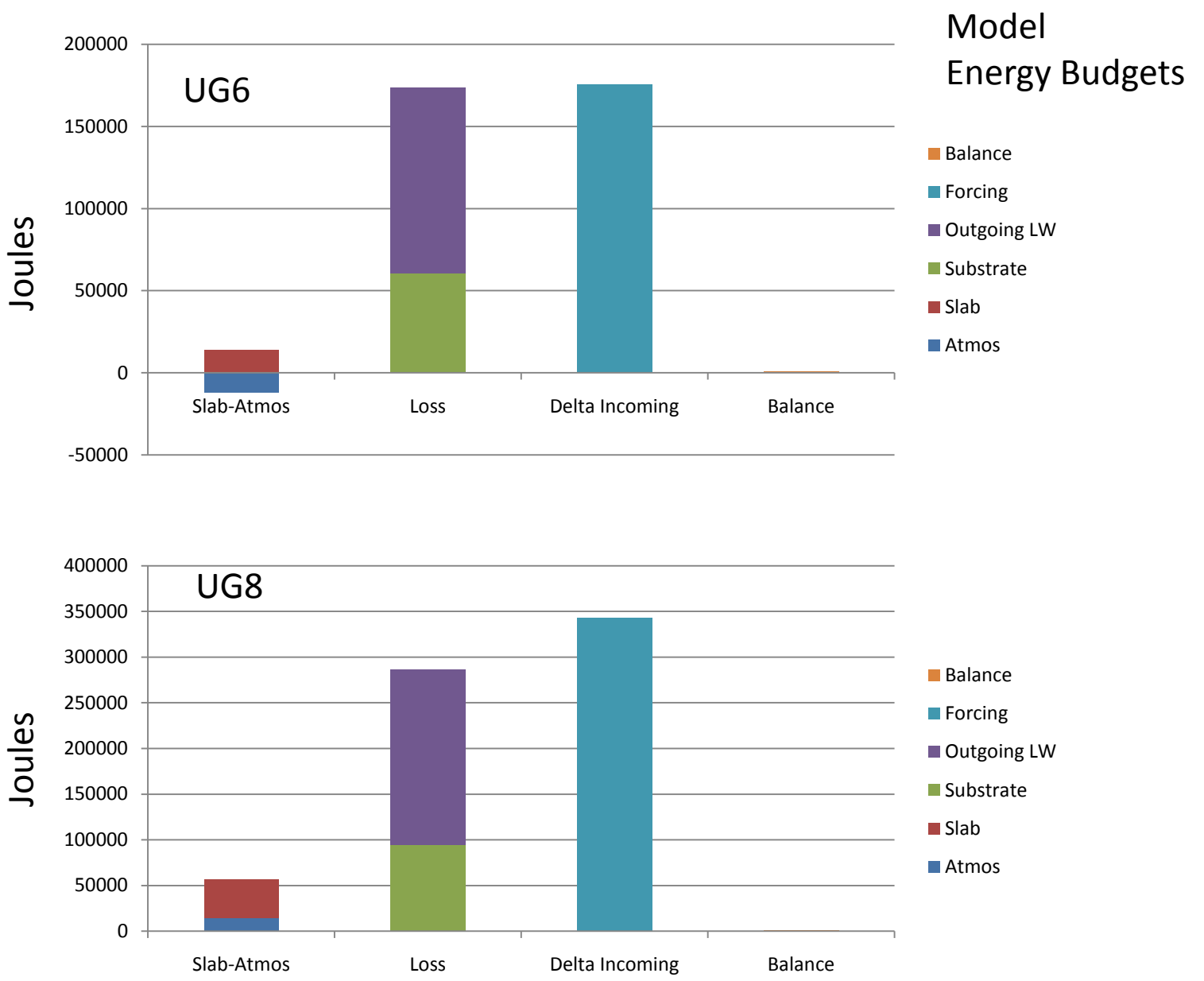

Figure 6: Model budget showing disposition of the added longwave energy (4.8Wm^{-2}) after 12 hours of simulation for the UAH model for the case of no clear air radiative forcing.

$$\Delta T = \frac{\Delta H}{\rho c p \Delta h}$$

ΔT = Temperature change

ΔH = Heat Increment

Δh = Boundary Layer Height

For boundary layer depth of 100 m and ΔH = 200,000J then ΔT=1.6 K

But only 14100J go into heating atmosphere then ΔT=0.11 K– how can the 1st level model temperature increase by 1.5 K ?

UAH

Answer lies in the redistribution of heat conjectured by Walters et al. 2007 from the dynamical system model.

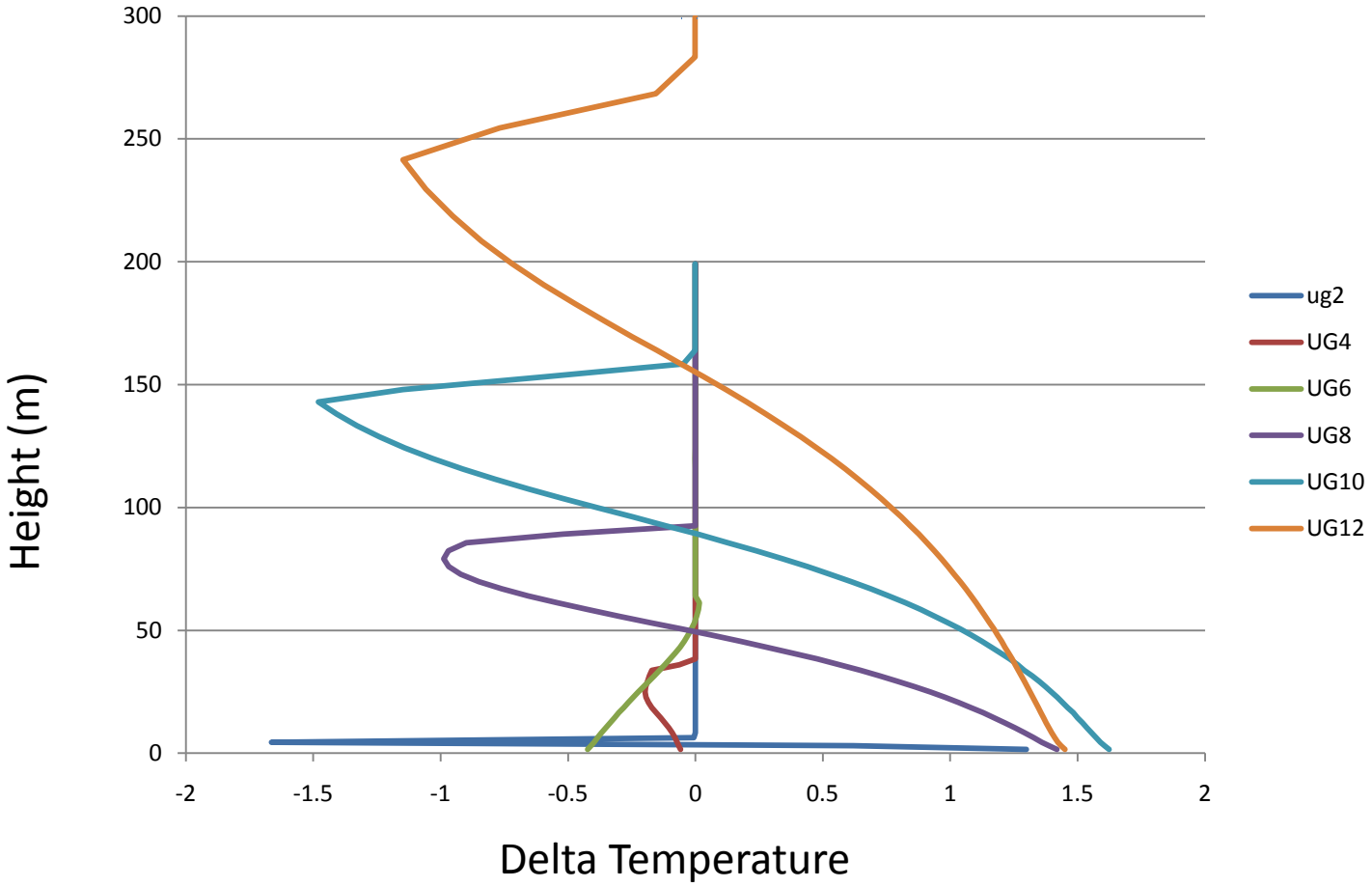

Figure 7: Difference in vertical profile between added GHG energy and base case from UAH for the case with no clear air radiative cooling.

Original Soil No Rad EM

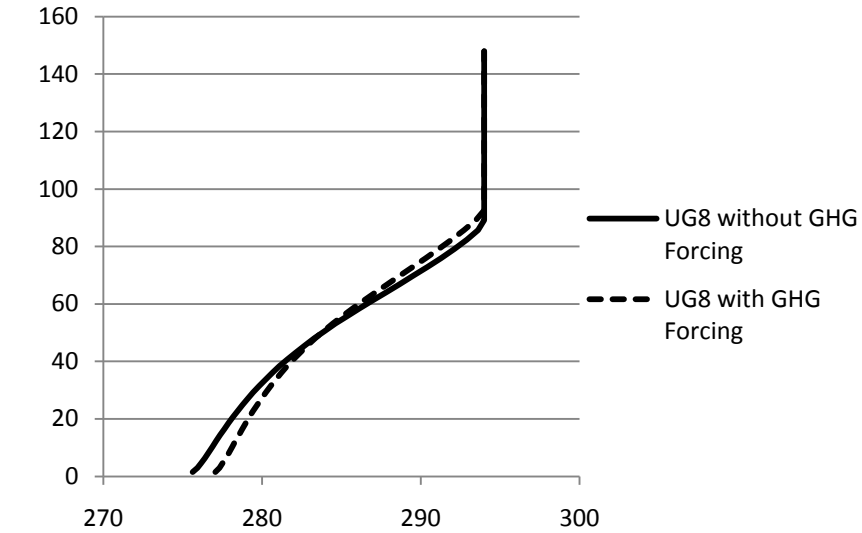

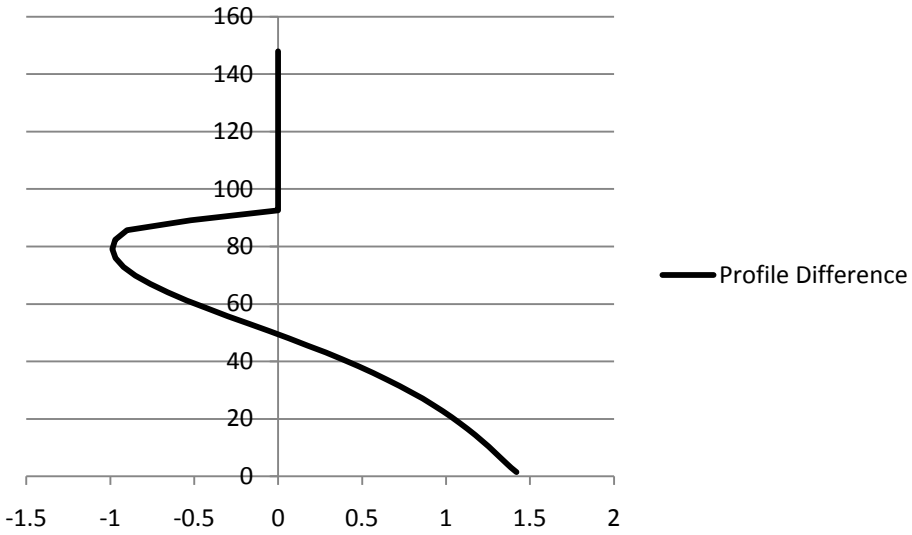

Figure 8: Expanded view of the difference in profile between the case of added GHG energy and base case for a geostrophic wind of 8 m/s.

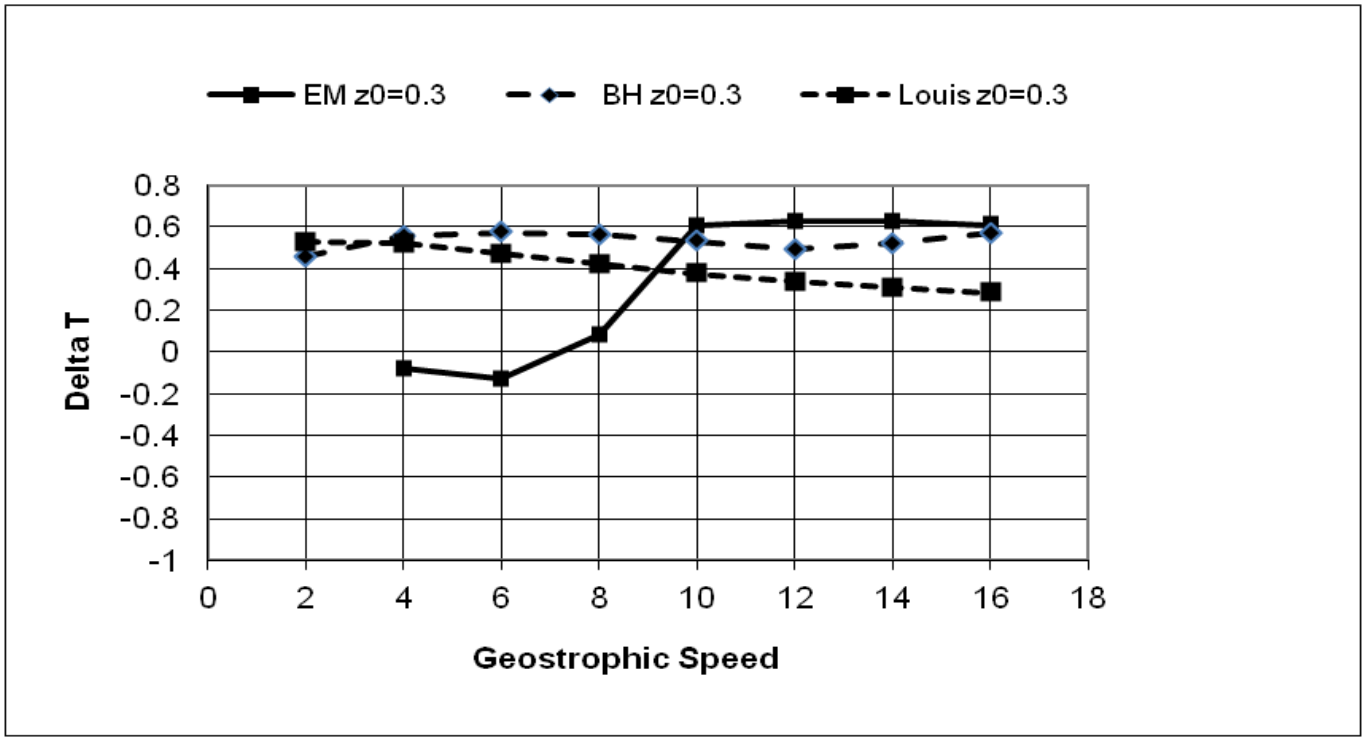

Figure 11: Differential heating for the case with clear air radiational forcing added radiative energy minus base case versus wind speed for different stability functions.

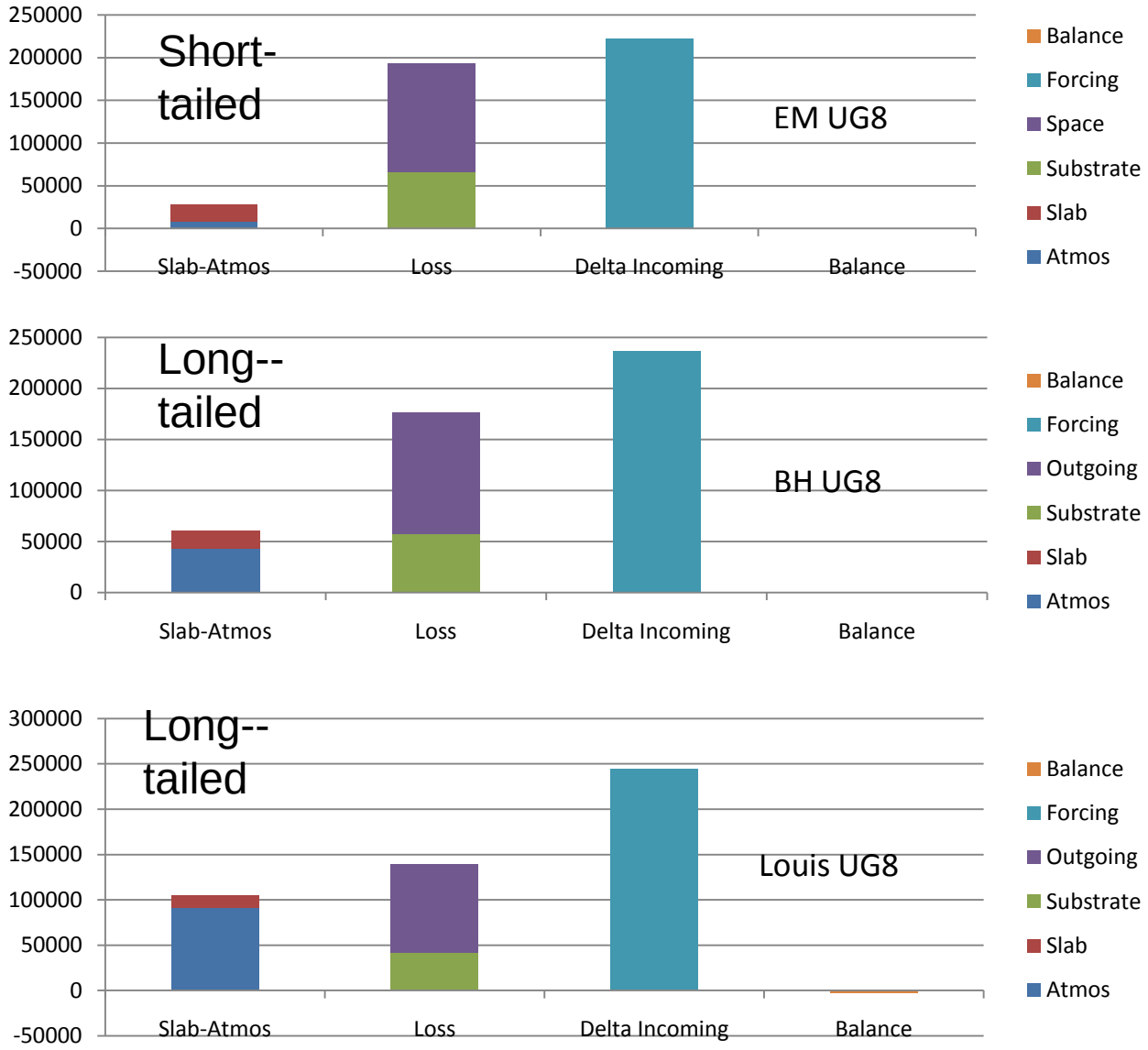

Figure 12: Model budget showing disposition of added longwave energy (4.8Wm^{-2}) after 12 hours of simulation for the UAH model for the case of with clear air radiative forcing for the England-McNider (EM), Beljaars-Holtslag (BH) and Louis stability function.

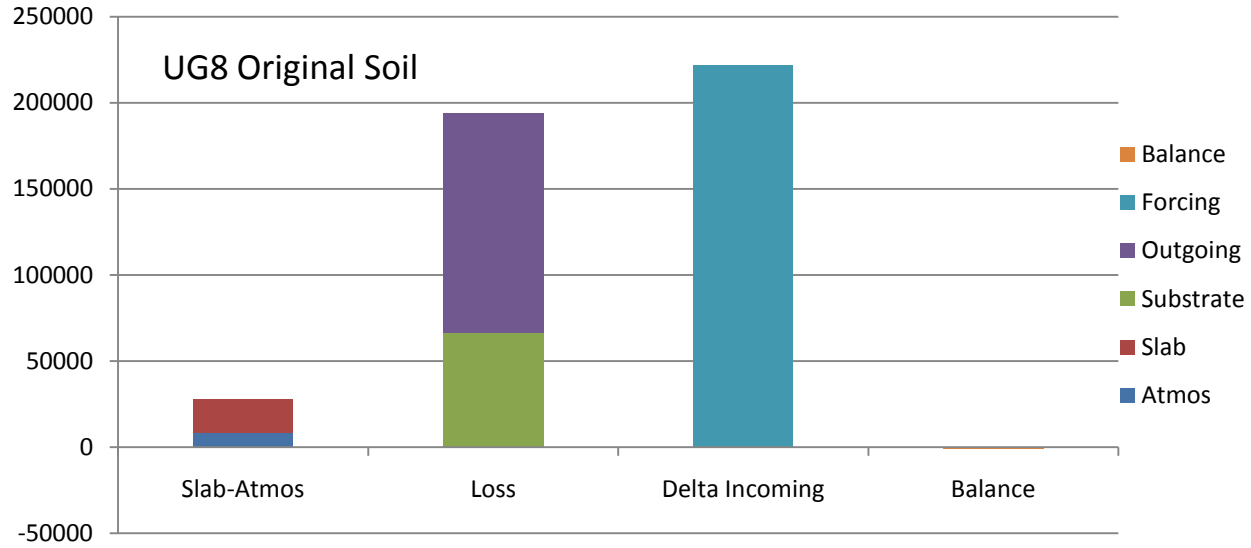
UG8 Original Soil
250000
200000
150000
100000
50000
0
-50000
Slab-Atmos
Loss
Delta Incoming
Balance
Balance
Forcing
Outgoing
Substrate
Slab
Atmos

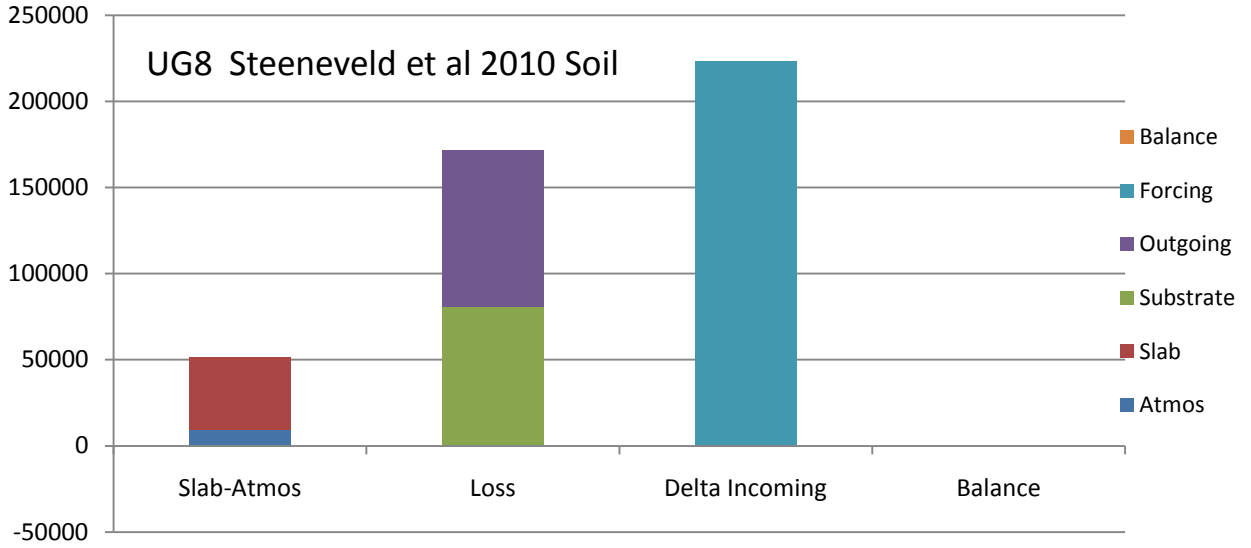
UG8 Steeneveld et al 2010 Soil
250000
200000
150000
100000
50000
0
-50000
Slab-Atmos
Loss
Delta Incoming
Balance
Balance
Forcing
Outgoing
Substrate
Slab
Atmos

UAH

Conclusions

The positive feedback due to a redistribution of heat when the SBL is destabilized by added downward radiation may be part of the reason for the differential rise in observed minimum temperatures.

The models/processes presented here that have increased temperature of 0.5-1.0K would explain a significant part of the differential minimum temperature warming.

Global models don't have the mechanisms or resolution to capture this feed back.

Downward radiation by aerosols which is also not handled well in GCMs may play a major role in the warming of minimum temperatures.

UAH

Recommendations

Understanding trends in minimum temperatures is important to understanding climate change. How much can we trust SBL models to respond correctly to added radiation or other changes (land use)?

GABLS should test the sensitivity of the SBL to added downward radiation or land-use parameters as its next model inter-comparison study.

GABLS-2 or GABLS-3 could be used as the control framework.

UAH

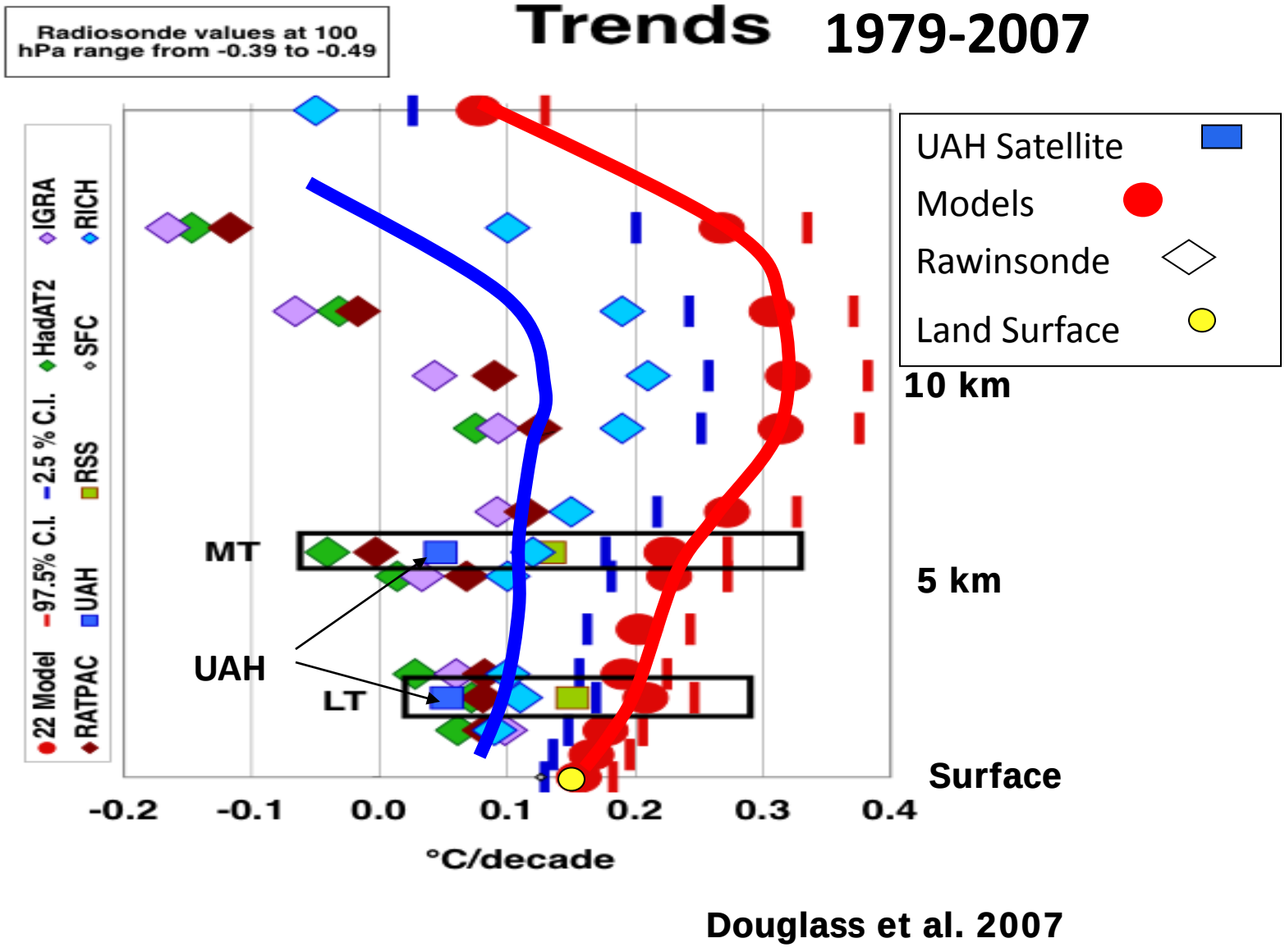
Radiosonde values at 100 hPa range from -0.39 to -0.49
Trends 1979-2007
22 Model
97.5% C.I.
2.5 % C.I.
HadAT2
IGRA
RICH
RATPAC
UAH
RSS
SFC
UAH Satellite
Models
Rawinsonde
Land Surface
10 km
5 km
Surface
MT
UAH
LT
-0.2
-0.1
0.0
0.1
0.2
0.3
0.4
°C/decade
Douglass et al. 2007

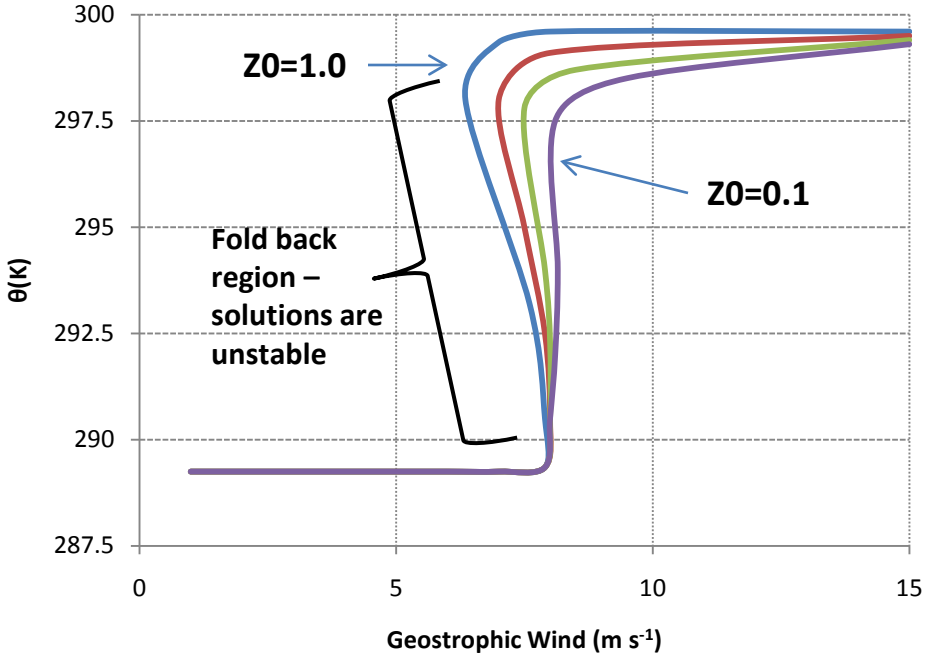
300
297.5
295
292.5
290
287.5
θ(K)
0
5
10
15
Geostrophic Wind (m s-1)
Z0=1.0
Z0=0.1
Fold back region – solutions are unstable

$$\Delta T = \frac{\Delta H}{\rho cp \Delta h}$$

ΔT = Temperature change

ΔH = Heat Increment

Δh = Boundary Layer Height

If heat input is the same then deeper boundary layers would warm at a greater rate

But Steeneveld et al 2010 showed that the heat input itself is a function of surface fluxes

UAH

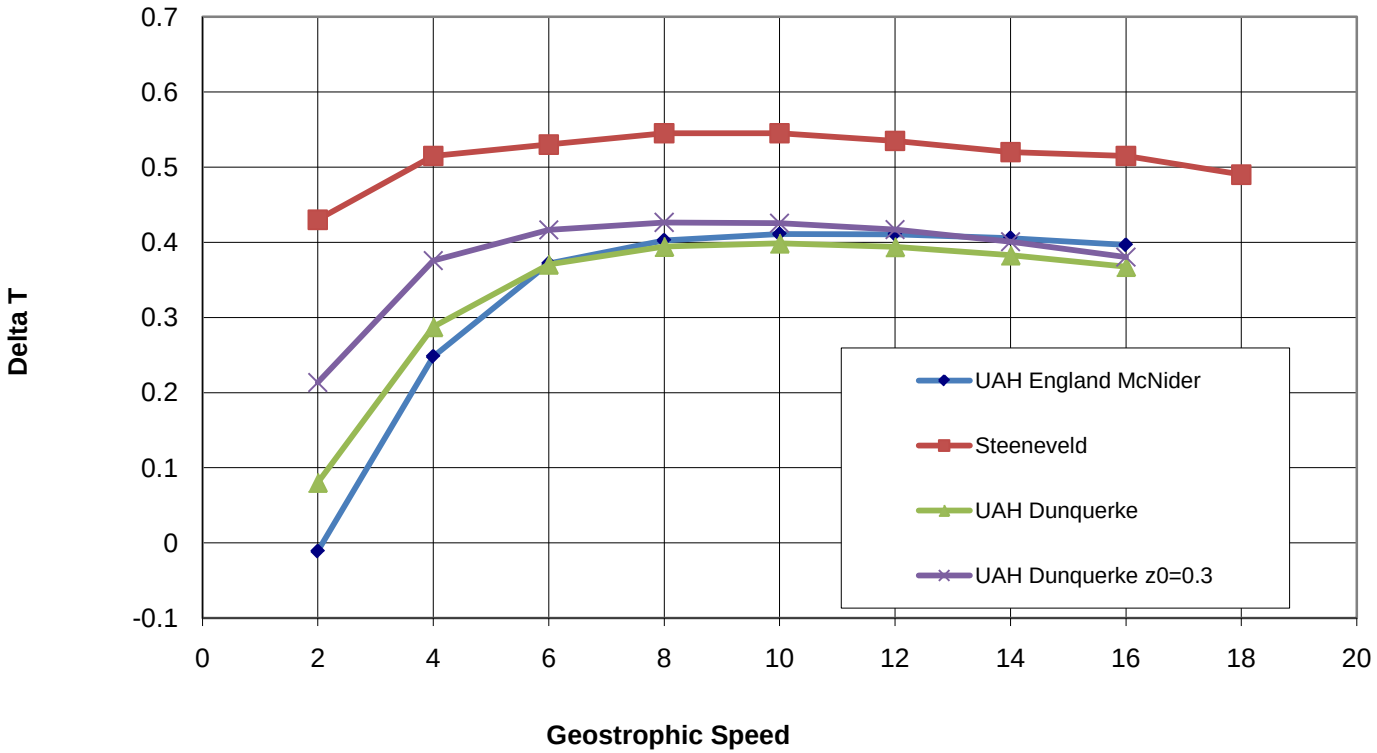

Figure 13: Differential heating - added GHG energy – base case versus wind speed for the Steeneveld soils case with clear air radiational forcing.

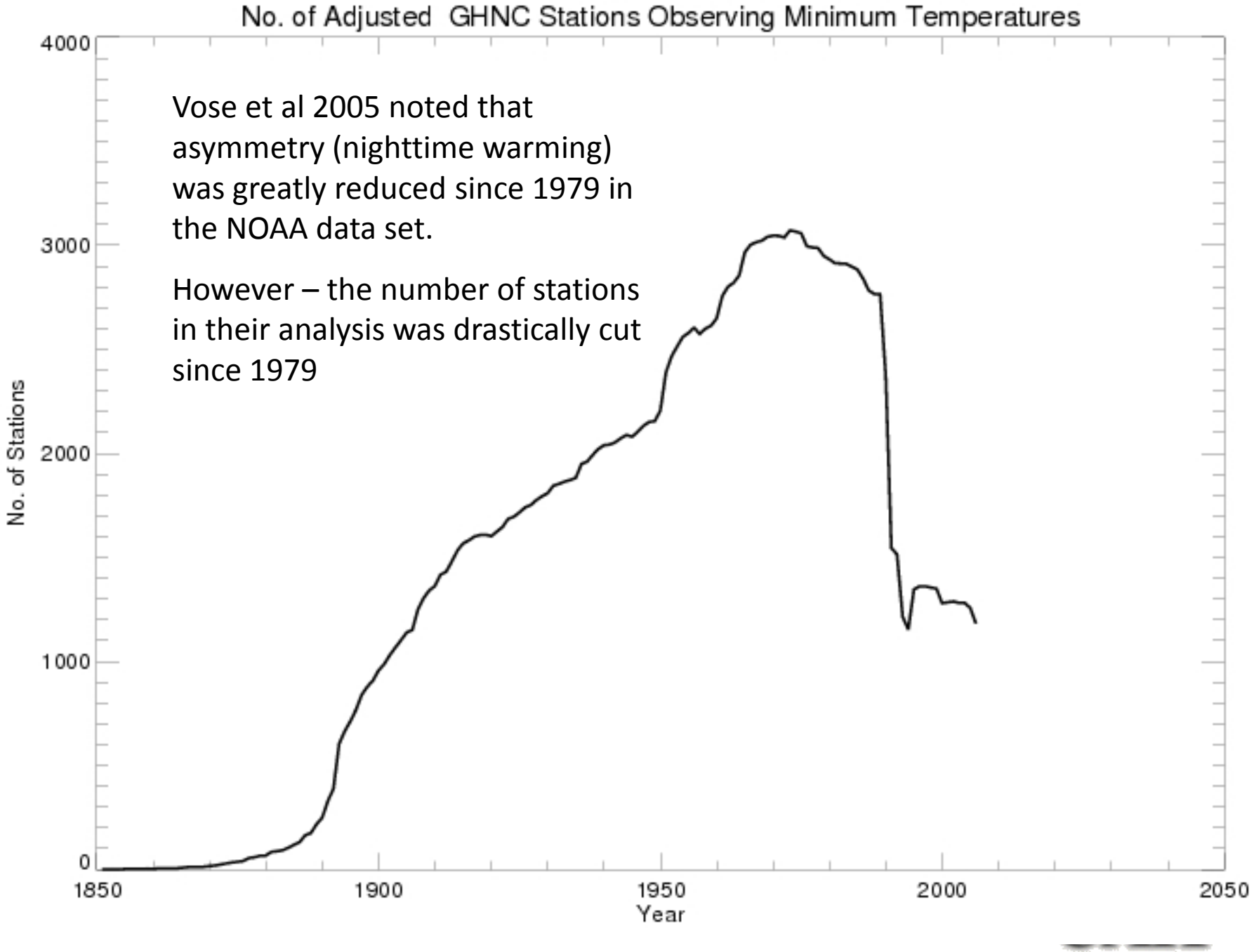
No. of Adjusted GHNC Stations Observing Minimum Temperatures
Vose et al 2005 noted that asymmetry (nighttime warming) was greatly reduced since 1979 in the NOAA data set.
However – the number of stations in their analysis was drastically cut since 1979
No. of Stations
4000
3000
2000
1000
0
1850
1900
1950
2000
2050
Year

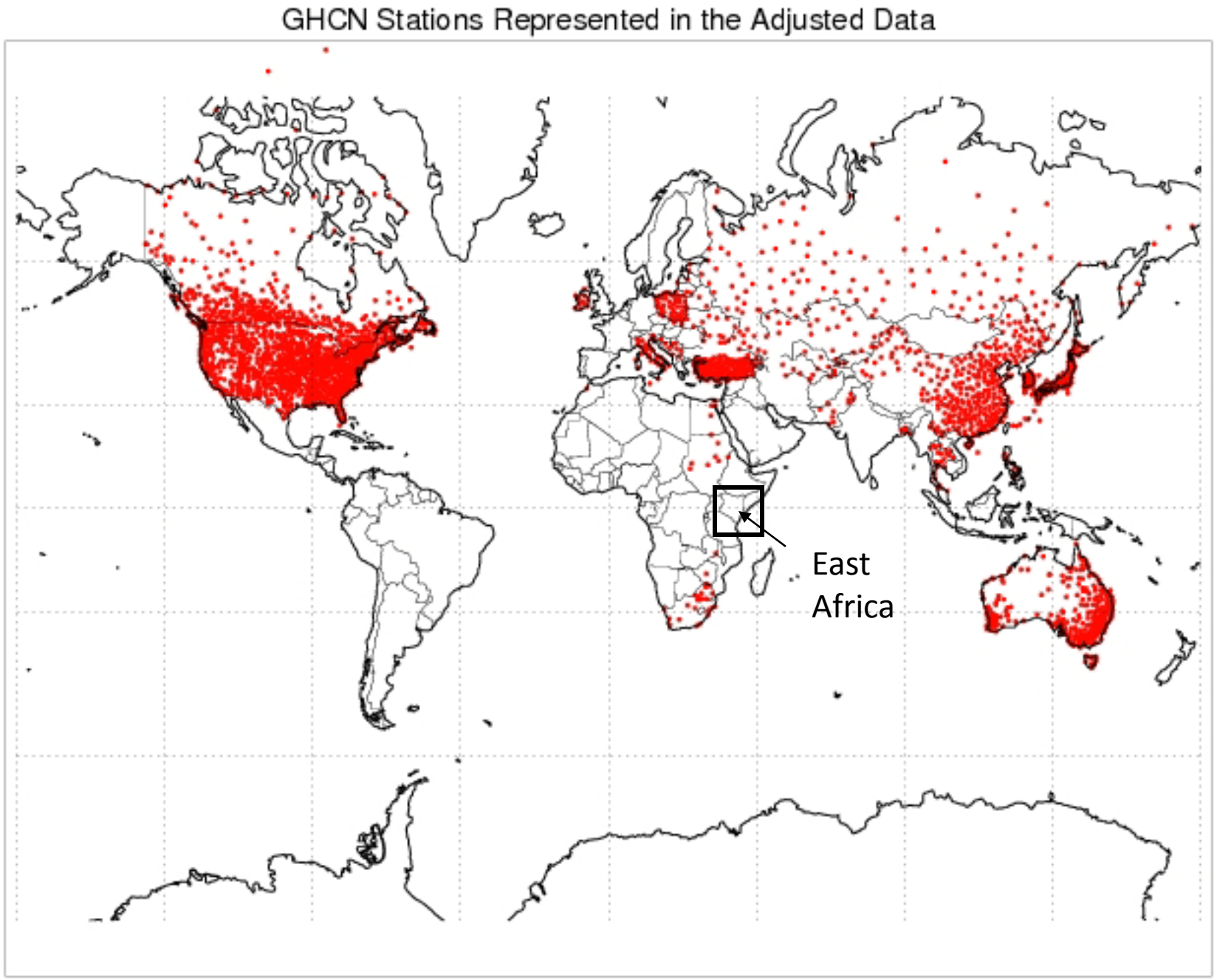
GHCN Stations Represented in the Adjusted Data
East
Africa

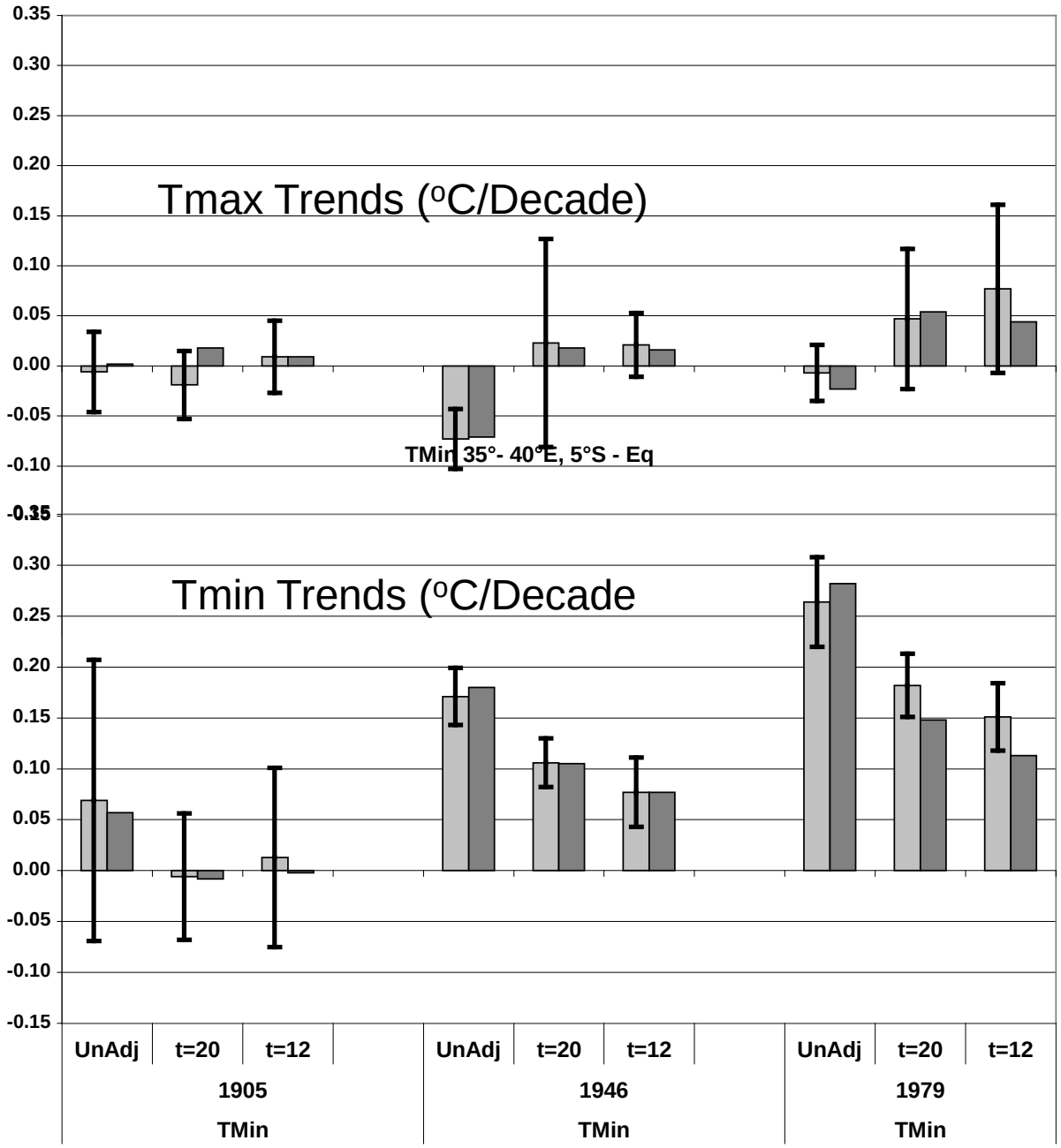
Tmax Trends (°C/Decade)
TMin 35°- 40°E, 5°S - Eq
Tmin Trends (°C/Decade
0.35
0.30
0.25
0.20
0.15
0.10
0.05
0.00
-0.05
-0.10
-0.15
UnAdj
t=20
t=12
1905
TMin
1946
1979

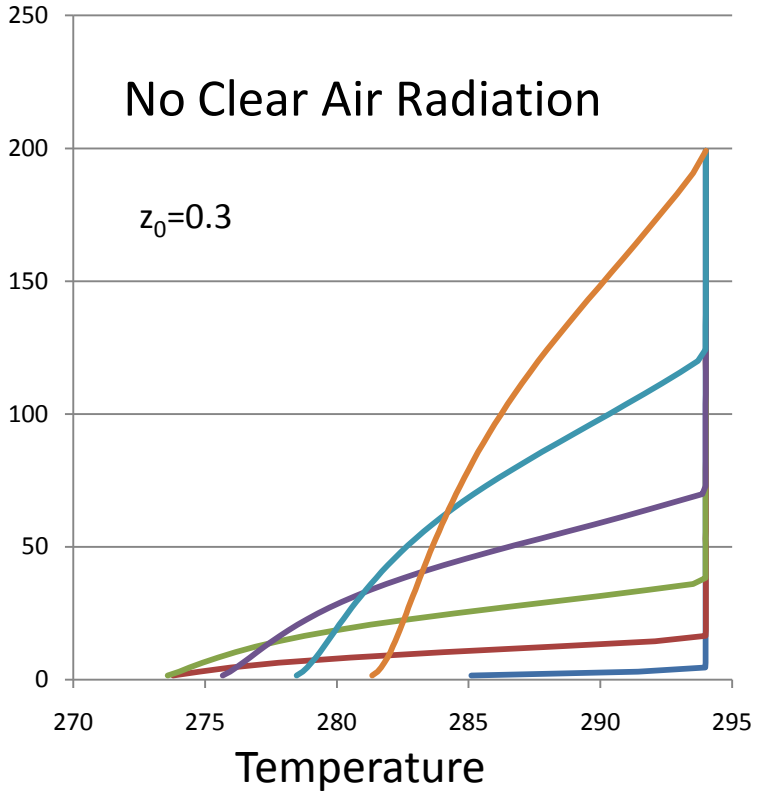
No Clear Air Radiation
z_0=0.3
250
200
150
100
50
0
270
275
280
285
290
295
Temperature

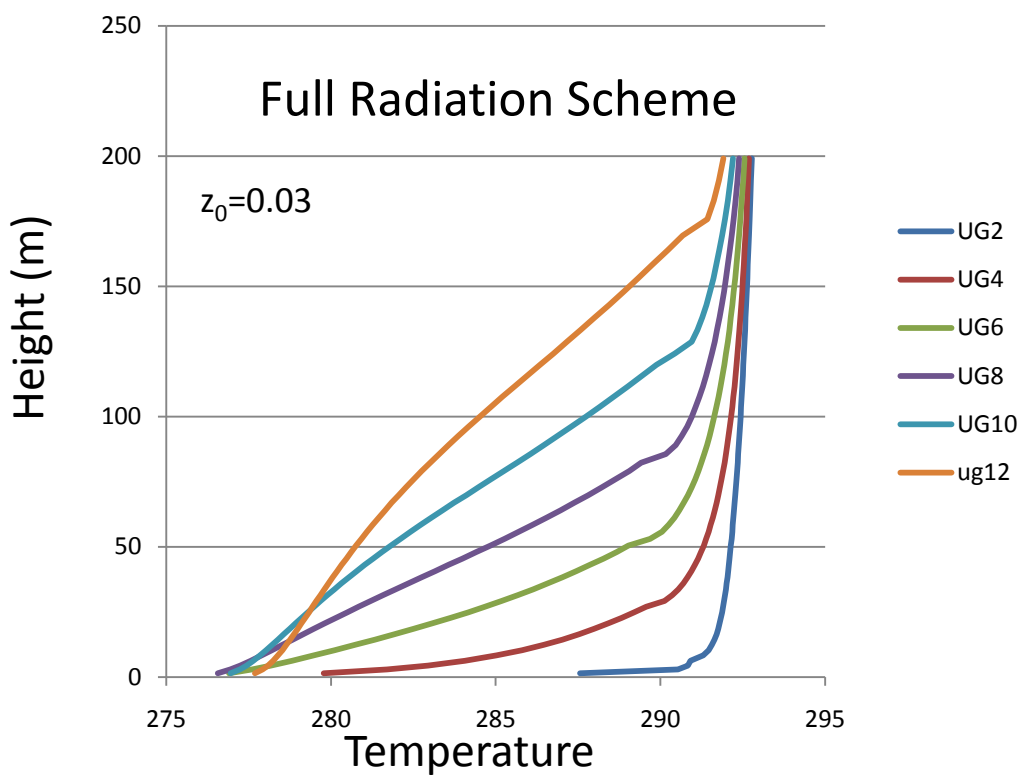
Full Radiation Scheme
z_0=0.03
Height (m)
250
200
150
100
50
0
275
280
285
290
295
Temperature
UG2
UG4
UG6
UG8
UG10
ug12

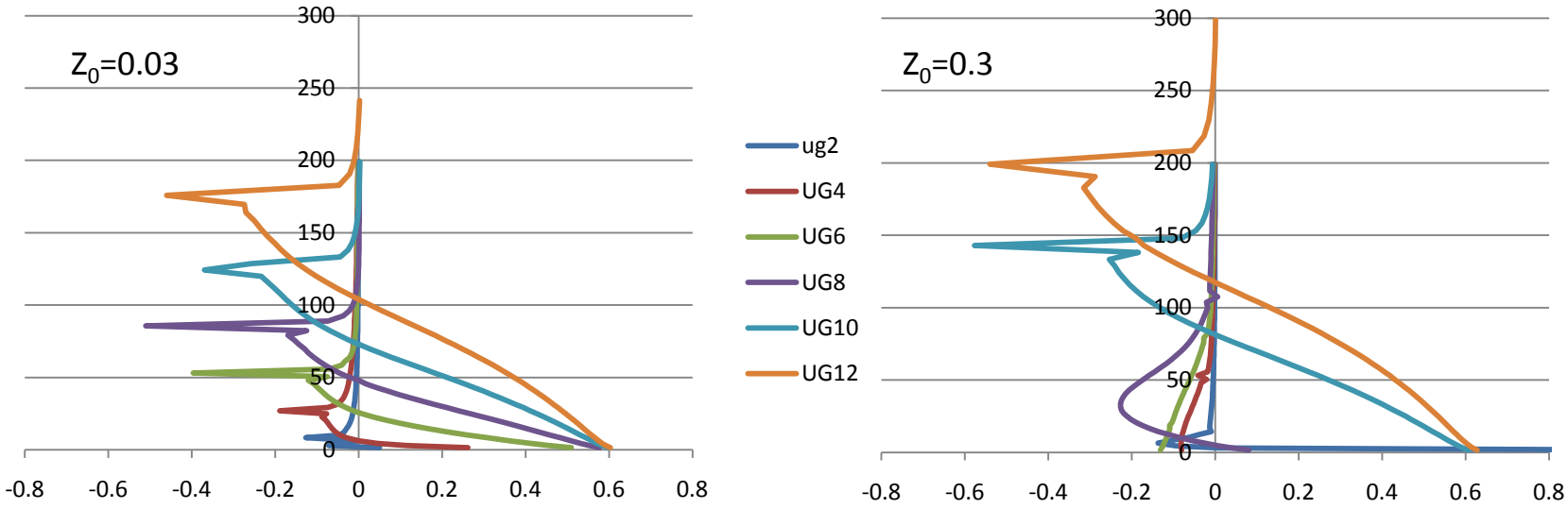

Figure 20: Difference in vertical profile between added GHG energy and base case from UAH for the case with clear air radiative cooling for two different roughness values.